Biogeosciences Discuss., https://doi.org/10.5194/bg-2018-88
Manuscript under review for journal Biogeosciences
Discussion started: 1 March 2018

Biogeosciences Discussions Open Access EGU

A niche comparison of *Emiliania huxleyi* and *Gephyrocapsa oceanica* and potential effects of climate change

Natasha A Gafar[1] and Kai G Schulz[1]

[1]Centre for Coastal Biogeochemistry, School of Environment Science and Engineering, Southern Cross University, Lismore, NSW 2480, Australia

Correspondence: Natasha Gafar (n.gafar.10@student.scu.edu.au)

Abstract. Coccolithophore responses to changes in carbonate chemistry speciation such as CO_2 and H^+ are highly modulated by light intensity and temperature. Here we fit an analytical equation, accounting for simultaneous changes in carbonate chemistry speciation, light and temperature, to published and original data for *Emiliania huxleyi*, and compare the projections with those for *Gephyrocapsa oceanica*. Based on our analysis, the two most abundant coccolithophores in today's oceans appear to be adapted for a similar fundamental light niche but slightly different ones for temperature and CO_2, with *E. huxleyi* having a tolerance to lower temperatures and higher CO_2 levels than *G. oceanica*. Based on growth rates, a dominance of *E. huxleyi* over *G. oceanica* is projected below temperatures of 22°C at current atmospheric CO_2 levels. This is similar to a global surface sediment compilation of *E. huxleyi* and *G. oceanica* coccolith abundances suggesting temperature dependent dominance shifts. For a future RCP 8.5 climate change scenario (1000 μatm fCO_2 and + 4.8°C) we project a niche contraction for *G. oceanica* to regions of even higher temperatures. Finally, we compare satellite derived particulate inorganic carbon estimates in the surface ocean with a recently proposed metric for potential coccolithophore success on the community level i.e. the temperature, light and carbonate chemistry dependent $CaCO_3$ production potential (CCPP). Excluding the Antarctic province from the analysis we found a good correlation between CCPP and satellite derived PIC in the other regions with an R^2 of 0.73 for Austral winter/Boreal summer and 0.85 for Austral summer/Boreal winter.

1 Introduction

Since the Industrial Revolution in the late 18th century, burning of fossil fuels, as well as wide scale deforestation have contributed to significant increases in atmospheric carbon dioxide, CO_2 (IPCC, 2013a). Depending upon the decisions in the next few decades, atmospheric CO_2 levels are projected to reach between 420 μatm (RCP2.6 scenario) and 985 μatm (RCP8.5 scenario) by 2100 (Caldeira and Wickett, 2005; Orr et al., 2005; IPCC, 2013a). To date approximately one third of the anthropogenic carbon emissions have been absorbed by the world's oceans (Sabine et al., 2004). As atmospheric partial pressures of CO_2 (pCO_2) increase, CO_2 concentrations in the surface ocean also increase, resulting in increased bicarbonate and hydrogen ions but also in decreased carbonate ion concentrations and pH (Doney et al., 2009; Schulz et al., 2009). These changes, often termed ocean carbonation and acidification, can have both positive and negative effects for different phytoplankton species and

Biogeosciences Discuss., https://doi.org/10.5194/bg-2018-88
Manuscript under review for journal Biogeosciences
Discussion started: 1 March 2018

groups (e.g. Engel et al. 2005; Feng et al. 2010; Moheimani and Borowitzka 2011; Endo et al. 2013; Schulz et al. 2017).

Associated with rising pCO_2 is the phenomenon of global warming. Under current scenarios, ocean temperatures are projected to increase from 2.6 to 4.8°C by 2100 (IPCC, 2013b). Warming of the ocean is expected to enhance vertical stratification of the water column, resulting in a shoaling of the surface mixed layer and increasing overall light availability in the euphotic zone (Bopp et al., 2001; Rost and Riebesell, 2004; Lefebvre et al., 2012). While increased light intensity often accelerates growth in phytoplankton, excessive levels of light can cause damage to the photosynthetic apparatus thus decreasing growth (Powles, 1984; Zondervan et al., 2002).

Coccolithophores play an important role in the marine carbon cycle through the precipitation of calcium carbonate, via calcification and the formation and settling of coccolith aggregates, as well as inorganic carbon fixation by photosynthesis (Rost and Riebesell, 2004; Broecker and Clark, 2009; Poulton et al., 2007, 2010). It is well established that rising pCO_2 will have significant effects on coccolithophorid growth, calcification and photosynthetic carbon fixation rates (Riebesell et al., 2000; Bach et al., 2011; Raven and Crawfurd, 2012). Furthermore, it has been shown that the response to rising pCO_2 of both *Gephyrocapsa oceanica* and *Emiliania huxleyi* is strongly influenced by light intensity and temperature (Zondervan et al., 2002; Schneider, 2004; De Bodt et al., 2010; Sett et al., 2014; Zhang et al., 2015). However, to which degree species specific responses may shape individual distribution and abundance in the future ocean is far less clear.

This is because the distribution and abundance of a species is controlled by several factors. Firstly, each species has a specific range of environmental conditions under which they can successfully grow and reproduce called the fundamental niche. The fundamental niche describes the multi-dimensional combination of environmental conditions, such as temperature, light and pCO_2, required for survival of a species assuming no other species are present (Leibold, 1995). However, species do not exist in a vacuum and where the niche of a species overlaps with another species interactions such as competition for resources and predation can occur (Hutchinson, 1957; Leibold, 1995), resulting in the realised niche (Leibold, 1995; Zurell et al., 2016). Hence it is not only important to determine how environmental change shapes the fundamental niche of individual species, but also consider the impact of niche overlap of different species in shaping the realised niches and hence community composition.

In the present study, we therefore compare species specific sensitivities and responses to combined light, temperature and carbonate chemistry changes of two of the most abundant coccolithophores *Emiliania huxleyi* and *Gephyrocapsa oceanica*. For that purpose, *E. huxleyi* was grown at twelve pCO_2 levels and five light intensities and growth, photosynthetic carbon fixation and calcification rates were measured in response. These data were then combined with a previously published data set on temperature and CO_2 interaction (Sett et al., 2014) and fitted to an analytical equation describing the combined effects of changing carbonate chemistry speciation, light and temperature. The resulting projections are then compared to those previously published for *G. oceanica* (Gafar et al., 2018) in an attempt to assess their individual success and potential realised niche in a changing ocean.

Biogeosciences Discuss., https://doi.org/10.5194/bg-2018-88
Manuscript under review for journal Biogeosciences
Discussion started: 1 March 2018

2 Methods

2.1 Experimental set-up

Mono-specific cultures of the coccolithophore *E. huxleyi* (strain PML B92/11 isolated from Bergen, Norway) were grown in artificial seawater (ASW) at 20°C and a salinity of 35 across a pCO_2 (partial pressure of CO_2) gradient from ~25-7000 μatm. Light intensities were set to 50, 400 and 600 $\mu mol photons\, m^{-2} s^{-1}$ of photosynthetically active radiation (PAR) on a 16:8 h light-dark cycle in a Panasonic Versatile Environmental Test Chamber (MLR-352-PE). An additional set of cultures was also incubated at 1200 $\mu mol photons\, m^{-2} s^{-1}$ under a Philips SON-T HPS 600W light in a water-bath set to 20°C. Light intensities at each bottle position for all experiments were measured using a LI-193 spherical sensor (LI-COR). Cells were pre-acclimated to experimental conditions for 8-12 generations. To account for differences in growth rate between the extreme high/low CO_2 treatments and the intermediate CO_2 treatments, initial cell densities chosen between 20-80 cells ml^{-1}. Treatments were run using a dilute-batch culture setup, mixed daily and harvested before dissolved inorganic carbon (DIC) consumption exceeded 10%.

2.2 Media

Artificial seawater (ASW) with a salinity of 35 was prepared according to Kester et al. (1967). ASW was enriched with f/8 trace metals (EDTA bound Fe, Cu, Mo, Zn, Co, Mn) and vitamins (thiamine, biotin, cyanocobalamin) according to Guillard (1975), 64 $\mu mol\, kg^{-1}$ nitrate (NO_3^-), 4 $\mu mol\, kg^{-1}$ phosphate (PO_4^{3-}), 10 nmol kg^{-1} SeO_2 and 1 ml kg^{-1} of coastal seawater (collected at Shelly beach, Ballina, NSW, Australia) to prevent possible limitation by trace elements during culturing which had not been added to the artificial seawater mix. ASW medium was sterile-filtered (0.2 μm pore size, Whatman™ Polycap 75 AS) directly into autoclaved acclimation (0.5 L) or experimental (2 L) polycarbonate bottles (Nalgene®), leaving a small head-space for the adjustment of carbonate chemistry conditions.

2.3 Carbonate chemistry manipulation, measurements and calculation

Carbonate chemistry, i.e. total alkalinity (TA) and dissolved inorganic carbon (DIC), for each treatment was adjusted through calculated additions of hydrochloric acid (certified 3.571 mol L^{-1} HCl, Merck) and Na_2CO_3 (Sigma-Aldrich, TraceSELECT® quality, dried for 2 hours at 240°C). Samples for TA and DIC measurements were taken at the end of the experiment. TA samples were filtered through GF/F filters, stored in the dark at 4°C and processed within 7 days (Dickson et al. 2007 SOP 1). TA samples were measured by potentiometric titration using a Metrohm Titrino Plus automatic titrator with 0.05 mol kg^{-1} HCl as the titrant, adjusted to an ionic strength of 0.72 mol kg^{-1} with NaCl (Dickson et al. 2007 SOP 3b).

DIC samples were sterile filtered by gentle pressure filtration with a peristaltic pump (0.2 μm pore size polycarbonate, Sartorius) into glass stoppered 100 ml bottles (Schott Duran) with overflow of at least 50% of bottle volume similar to Bockmon and Dickson (2014), sealed without head-space and stored in the dark at 4°C until processing within 7 days. To determine DIC,

Biogeosciences Discuss., https://doi.org/10.5194/bg-2018-88
Manuscript under review for journal Biogeosciences
Discussion started: 1 March 2018

2 ml of sample was analysed on a Marianda AIRICA system by acidification with 10% phosphoric acid to convert all DIC into CO_2, followed by extraction with N_2 (5.0) and concomitant CO_2 analysis with an IR detector (LI-COR LI-7000 CO_2/H_2O analyser). Both TA and DIC measurements were calibrated against Certified Reference Materials (batches 139, 141, 150) following Dickson (2010). Initial DIC and TA concentrations were estimated by adding measured total particulate carbon build-up during incubations to measured final DIC, and double the particulate inorganic carbon build-up during incubations to measured final TA concentrations. Carbonate chemistry speciation for each treatment was calculated from mean TA, mean DIC, measured temperature, salinity and [PO_4^{3-}] using the program CO2SYS (Lewis et al., 1998), the dissociation constants for carbonic acid determined by Lueker et al. (2000), K_S for sulphuric acid determined by Dickson et al. (1990) and K_B for boric acid following Uppström (1974).

2.4 Particulate organic and inorganic carbon

Sampling started approximately two hours after the onset of the light period and lasted no longer than 3 hours. Duplicate samples for total and particulate organic carbon (TPC and POC) were filtered (-200 mbar) onto GF/F filters (Whatmann, pre-combusted at 500°C for 4 hours) and stored in glass petri-dishes (pre-combusted at 500°C for 4 hours) at -20°C until analysis. POC filters were placed in a desiccator above fuming (37%) HCl for 2 hours to remove all particulate inorganic carbon (PIC). All filters were dried overnight at 60°C, and analysed for carbon content and corresponding isotopic signature according to Sharp (1974) on an elemental analyser (Flash EA, Thermo Fisher) coupled to an isotope ratio mass spectrometer (IRMS, Delta V plus, Thermo Fisher). Particulate inorganic carbon (PIC) was calculated by subtracting measured POC from TPC.

2.5 Growth

Cell densities were measured every 3-4 days after the commencement of the experiment using a flow cytometer (Becton Dickinson FACSCalibur) on high flow settings (58 μl/minute) for two minutes per measurement. Living cells were detected by their red autofluorescence in relation to their orange fluorescence in scatter plots (FL3 vs. FL2). At some extreme CO_2 levels there was an initial lag phase and therefore growth rates were calculated from densities only during the exponential part of the growth phase. After disregarding lag phase measurements, the majority of treatments had only two to three data-points in the exponential phase. As a result, specific growth rates were calculated as:

$$\mu = \frac{\ln(C_f) - \ln(C_0)}{d} \quad (1)$$

where C_f represents cell densities at time of sampling, C_0 represents cell densities at the beginning of the exponential growth phase, and d is the duration of the exponential phase in days. Calcification and photosynthetic rates were calculated by multiplying cellular PIC and POC quotas with respective growth rates.

Biogeosciences Discuss., https://doi.org/10.5194/bg-2018-88
Manuscript under review for journal Biogeosciences
Discussion started: 1 March 2018

2.6 Fitting procedure

Coccolithophore metabolic rate (MR) responses of growth, calcification and photosynthetic carbon fixation to combined changes in temperature, light and carbonate chemistry speciation can be described as follows (Gafar et al., 2018).

$$\mathrm{MR}(T,I,S,H) = \frac{\mathrm{k_1SIT}}{\mathrm{k_2HT + k_3SHT + k_4I + k_5SI + SIT + k_6SHI^2T^2}} \quad (2)$$

where, k_1 (pg C cell^{-1} day^{-1} or day^{-1}), k_2 (μmol photons m^{-2}s^{-1}), k_3 (kg mol^{-1} μmol photons m^{-2} s^{-1}), k_4 (mol kg^{-1} °C), k_5 (°C), k_6 (kg mol^{-1} μmol photons^{-1} m^{2}s °C^{-1}) are fit coefficients, and MR(T,I,S,H) is the metabolic rate of photosynthesis, calcification or growth dependent on temperature (T), light intensity (I), substrate (S = [CO_2] + [HCO_3^-]) and [H^+] (H). Inputs to the equation consisted of calculated CO_2, HCO_3^- and H^+ (H in total scale) concentrations, as well as measured metabolic rates, and light (I) and temperature (T) levels of all treatments (please see below for information on temperature and light transforms).

Data from this study (Tables S1, S2) and Sett et al. (2014) were fitted to Eq. (2) using the non-linear regression fit procedure nlinfit in MATLAB (the Mathworks). The reason only these studies were chosen, from the multitude of *E. huxleyi* datasets, is because 1) they use the same strain (PML B92/11), 2) they have the same nutrient conditions and 3) they use the same carbonate chemistry manipulation methods. Nevertheless, the two chosen studies provided light (six levels) and temperature (three levels) interactions over a broad carbonate chemistry speciation range. It is noted that in both studies the carbonate chemistry system is coupled, meaning that a change in CO_2 results in a change in pH. This method reflects the changes in carbonate chemistry speciation due to ongoing ocean acidification (Bach et al., 2011, 2013). However, some studies have examined the effects of decoupled carbonate chemistry where CO_2 is changed at a constant pH. This approach is used to tease apart the independent effects of H^+ and CO_2 on physiological responses (see Bach et al. 2013). While Eq. (2) can also be used to explain responses under decoupled carbonate chemistry conditions (see Gafar et al. 2018 for details), the fit obtained here is only valid for coupled CO_2/pH changes as no data from decoupled experiments (i.e. Bach et al. 2011) has been used. The reason for this being that Bach et al. (2011) does not contain data of temperature, light and carbonate chemistry interactions.

2.7 Temperature and light transformations

To reduce skew and to better accommodate certain features (i.e. light and temperature inhibition and limitation) both temperature and light data were transformed. Light data was square root transformed with light $(\mathrm{I}) = \sqrt{\mathrm{PFD}}$, where PFD is the photon flux density ($\mu\mathrm{mol\,photons\,m^{-2}s^{-1}}$) of an incubation. To accommodate for known temperature inhibition below 2°C and above 30°C (Rhodes et al., 1995; van Rijssel and Gieskes, 2002; Helm et al., 2007; Zhang et al., 2014) at a much narrower experimental range (10-20°C), the upper and lower limits for *E. huxleyi* growth were added into the equation with a general transform of $\mathrm{T} = (\mathrm{T_t} - 2) \times (30 - \mathrm{T_t})$, where T_t is the temperature of an incubation. To accurately express the onset of high temperature inhibition, the transform was further modified with a square root transform to give $\mathrm{T} = (\mathrm{T_t} - 2) \times \sqrt{(30 - \mathrm{T_t})}$.

Biogeosciences Discuss., https://doi.org/10.5194/bg-2018-88
Manuscript under review for journal Biogeosciences
Discussion started: 1 March 2018

This transform produces reasonable results when compared to the Eppley temperature envelope curve and the Norberg model (see Gafar et al. 2018).

2.8 Physiological rate response parameter estimations to changes in carbonate chemistry, temperature and light

Equation (2) was used to assess the combined effects of carbonate chemistry, temperature and light on growth, calcification and photosynthetic carbon fixation rates, with a focus on general physiological features, such as limitation and inhibition, as well as how much variability could be explained. For growth, photosynthetic carbon fixation and calcification rates optimum CO_2 concentrations for maximum production rates (V_{max}) and half saturation values were calculated at each experimental light and temperature level. $K\frac{1}{2}$ values consisted of: $K\frac{1}{2}_{CO_2}sat$ which is the CO_2 concentration (at certain T and I) at which rates are saturated to half the maximum, and $K\frac{1}{2}_{CO_2}inhib$, which is the CO_2 concentration (at certain T and I) at which high proton concentrations reduce physiological rates to half the maximum. Fitting results (R^2, fit coefficients, p-values, F-values and degrees of freedom), as well as V_{max}, $K\frac{1}{2}$ and CO_2 optima are presented in Tables 1, 2 and 3. Species specific differences in response to changing carbonate chemistry, temperature and light were assessed by comparing the above fit to that recently produced for *Gephyrocapsa oceanica* (Gafar et al., 2018).

2.9 Niche comparison

To examine the potential of ongoing ocean change to influence realised niches and hence individual success, ranges for light and temperature where both *Emiliania huxleyi* and *Gephyrocapsa oceanica* might be expected to co-exist were selected (i.e. 50-1000 $\mu\mathrm{mol\,photons\,m^{-2}s^{-1}}$ and 8-30°C). *E. huxleyi* and *G. oceanica* were chosen for comparison as they are currently the only two species with response data over a range of carbonate chemistry, temperature and light conditions. Growth rates were selected as the point of comparison because they can be used as a measure of relative abundance and therefore dominance of a species, and because growth rates largely control carbon fixation rates. To assess competitive ability, and the potential realised niche, the difference in growth rates between the species was visualised using contour plots.

The effect of temperature on growth rates and hence potential dominance was then compared to phytoplankton community data from global surface sediment samples above the lysocline (McIntyre and Bé, 1967; Chen and Shieh, 1982; Roth and Coulbourn, 1982; Knappertsbusch, 1993; Andruleit and Rogalla, 2002; Boeckel et al., 2006; Fernando et al., 2007; Saavedra-Pellitero et al., 2014). As *E. huxleyi* and *G. oceanica* have similar average numbers of coccoliths per cells, 28 and 21, respectively (Samtleben and Schroder, 1992; Knappertsbusch, 1993; Baumann et al., 2000; Boeckel and Baumann, 2008; Patil et al., 2014), the abundance ratio of *E. huxleyi* to *G. oceanica* coccoliths was here assumed to be a suitable proxy for species dominance. It is noted that *E. huxleyi* has been found to produce excess coccoliths towards the end of blooms when inorganic nutrients become limiting for cellular growth (Balch et al., 1992; Holligan et al., 1993; Paasche, 1998), which would result in an over-estimate of *E. huxleyi* dominance in our study. Nevertheless, given that the coccoliths ratio varies orders of magnitude in modern marine sediments, none of our general conclusions should be affected. Temperature for each sampling site was retrieved from the NOAA 1° resolution annual temperature climatology (Boyer et al., 2013).

Biogeosciences Discuss., https://doi.org/10.5194/bg-2018-88
Manuscript under review for journal Biogeosciences
Discussion started: 1 March 2018

2.10 Global calcium carbonate production potential

While our fit equation has previously explained variability in lab experiments quite well (Gafar et al., 2018), natural systems are much more complex, with the interactions of dozens of variables including temperature, light, nutrients, predation and competition all influencing productivity (Behrenfeld, 2014). As such we wanted to examine how our, relatively simple, equation projections of productivity compared to coccolithophorid productivity patterns observed in natural systems. Productivity can be defined in a few ways, traditionally, changes in cellular calcification rates, in response to ocean change, have been used as indicator for the potential success of coccolithophores in the future ocean. However, the exponential nature of phytoplankton growth amplifies even small differences in cellular growth rates, when applied on the community level. For instance, a phytoplankton bloom occurring over one week at a growth rate of 1.0 d^{-1} and a starting cell density of 50 cells ml^{-1} would lead to a peak density of about 55,000 cells ml^{-1}. This is in stark contrast to conditions where growth is only 10% lower as peak cell densities, and hence biomass and PIC standing stock, will only be half.

Recently, a new metric was proposed, the $CaCO_3$ production potential (CCPP) which 1) should be a better representation of potential coccolithophore success on the community level and 2) can be tested against modern observations of surface ocean $CaCO_3$ distribution. CCPP is defined as the amount of $CaCO_3$ produced within a week by a coccolithophore community (with a set starting cell count) for a certain environmental condition, calculated from Eq. (2) derived growth rates and inorganic carbon quotas. Inorganic carbon quotas are calculated as the quotient of calcification and growth rates. As CCPP is calculated from calcification and growth rates, it accounts for the individual effects of temperature, light and carbonate chemistry on growth rates and on carbon production. It was for these reasons that CCPP was the metric chosen for comparison.

Provided values for temperature, light, substrate (CO_2 + HCO_3^-) and hydrogen ion concentrations (H) for the surface mixed layer, coccolithophore $CaCO_3$ production potential can be projected for the world oceans. CCPP can then be cautiously evaluated against and compared to satellite derived global particulate inorganic carbon concentration estimates (PIC_s). As inorganic nutrients are a critical factor influencing phytoplankton abundance, and especially bloom formation, in the ocean (Browning et al., 2017) nitrate concentrations were also included in the analysis (for details see below). As a result, climatological datasets consisted of, World Ocean Atlas 2013 v2 (WOA) nitrate concentrations at 1° resolution (Boyer et al., 2013); SeaWiFS mixed layer depth (MLD 2° resolution) from de Boyer Montégut et al. (2004); surface photosynthetically available radiation (PAR $\mu mol photons\, m^{-2} s^{-1}$ 9 km resolution) from the Moderate Resolution Imaging Spectroradiometer (MODIS)-Aqua (NASA Goddard Space Flight Center, 2014b); diffuse attenuation coefficients at 490nm (9 km resolution) from Pascal (2013); and NOAA dissolved inorganic carbon, pCO_2, pH (total scale), [CO_3^{2-}], temperature and salinity (4x5° resolution) from Takahashi et al. (2014). A 9 km resolution climatology for particulate inorganic carbon (PIC_s) concentration (mol PIC m^{-3}) was also retrieved from the Moderate Resolution Imaging Spectroradiometer (MODIS)-Aqua (NASA Goddard Space Flight Center, 2014a). Once acquired, all datasets were interpolated to a 1° resolution.

Biogeosciences Discuss., https://doi.org/10.5194/bg-2018-88
Manuscript under review for journal Biogeosciences
Discussion started: 1 March 2018

Hydrogen ion concentrations were calculated as $10^{-\mathrm{pH}}$, CO_2, after conversion of pCO_2 to fCO_2 as described in CO2SYS (Lewis et al., 1998), as [fCO_2]*K0 (with K0 being the temperature and salinity dependent Henry's constant), HCO_3^- as [HCO_3^-] = DIC - ([CO_2] + [CO_3^{2-}]), and substrate (S) as the sum of CO_2 and HCO_3^- concentrations. Mean mixed layer nitrate concentrations were calculated by determining concentrations for each depth and averaging from surface to the mixed layer depth for each grid cell. Mean mixed layer irradiance was calculated in one meter depth increments for each grid cell as

$$\mathrm{I} = \sum_{\mathrm{i}=1}^{\mathrm{MLD}} = \exp^{-\mathrm{k_d(i)}} * \mathrm{I_0} \tag{3}$$

where I is the average PAR ($\mu\mathrm{mol\,photons\,m^{-2}s^{-1}}$), k_d is the attenuation coefficient ($\mathrm{m^{-1}}$), MLD denotes the mixed layer depth in meters, and I_0 is the incident PAR at the surface ($\mu\mathrm{mol\,photons\,m^{-2}s^{-1}}$).

Global coverage of oceanic nutrient concentrations are often limited to only a few macro-nutrients (nitrate, silicate, phosphate). However, concentrations of these nutrients are often strongly correlated (e.g. phosphate and nitrate in Boyer et al. 2013). To ensure there was sufficient nutrients to support the level of production estimated by CCPP, we opted to use a single nutrient, i.e. nitrate, in combination with a simple scaling metric. First it was assumed that $CaCO_3$ is produced with a PIC:PON ratio of 6.625 for *E. huxleyi* and 13.25 for *G. oceanica* (based on Redfield proportions and PIC:POC ratios of one and two respectively). Hence, maximum $CaCO_3$ production potential ($CCPP_{max}$) in a grid cell would be 6.625 and 13.25 times the nitrate concentration for *E. huxleyi* and *G. oceanica* respectively. If estimated CCPP for a cell exceeded $CCPP_{max}$, and therefore the nitrate required to produce that much PIC, then it was replaced with the $CCPP_{max}$ value. If CCPP was less than C_{max} then no further changes were applied.

To ensure that mean global CCPP and mean global PIC_s would be of the same magnitude, starting cell counts for CCPP calculations were set at 1 $\mathrm{ml^{-1}}$ for *E. huxleyi* alone, 0.25 $\mathrm{ml^{-1}}$ for *G. oceanica* alone and 0.25 $\mathrm{ml^{-1}}$ for each species when combined. To allow comparison, CCPP and PIC_s were both converted to units of μmol PIC $\mathrm{L^{-1}}$. All data were then averaged for Austral summer/Boreal winter (December-February) and Austral winter/Boreal summer (June-August). Austral summer/Boreal winter and Austral winter/Boreal summer were chosen as they provide prominent differences between minimum and maximum PIC, while spring and autumn do not. A direct comparison between PIC_s and CCPP was achieved by splitting results into major ocean biogeographical provinces following Gregg and Casey 2007 with the single change of adjusting the Antarctic and the north ocean regions to start at 45° as in Longhurst 2007 rather than 40° (Figure S1). For each major province, the total amount of PIC_s and CCPP for all comparable grid cells were calculated for Austral summer/Boreal winter and Austral winter/Boreal summer. For comparison, values for each basin and season were then converted into percentages of annual global (global summer plus global winter) PIC_s or CCPP production. Agreement between the satellite and CCPP estimates was then assessed using a linear correlation.

Biogeosciences Discuss., https://doi.org/10.5194/bg-2018-88
Manuscript under review for journal Biogeosciences
Discussion started: 1 March 2018

3 Results

The fit equation (Eq. 2) was able to explain up to 85% of the variability in measured metabolic rates of *E. huxleyi* across a broad range of carbonate chemistry (25-4000 μatm), light (50-1200 $\mu\mathrm{mol\,photons\,m^{-2}s^{-1}}$) and temperature (10-20°C) conditions (Table 1).

3.1 Responses to changing carbonate chemistry: CO_2 and H^+

All rates had a similar optimum curve response to the broad changes in carbonate chemistry speciation (Figure 1) regardless of temperature and light intensities. Growth, calcification and photosynthetic carbon fixation rates required similar CO_2 concentrations to stimulate rates to half the maximum, $\mathrm{K}\frac{1}{2}_{CO_2}sat$ (Table 2, Table 3). Optimum CO_2 concentrations for calcification were slightly lower than for photosynthesis or growth (Table 2, Table 3). At CO_2 concentrations beyond the optimum, a much higher sensitivity to increasing [H^+], i.e. $\mathrm{K}\frac{1}{2}_{CO_2}inhib$ was observed for calcification than for photosynthesis or growth rates (Tables 2, 3 and Figures 1, 2).

3.2 Responses to temperature

The effect of temperature on rates was dependent upon CO_2, with the greatest effect observed at optimum CO_2 concentrations (Figure 1). Increasing temperature increased growth rates up to twofold, photosynthetic rates up to 43% and calcification rates up to 52% (Figure 1, Table 2) under optimal CO_2 concentrations. CO_2 half saturation concentrations ($\mathrm{K}\frac{1}{2}_{CO_2}sat$) were insensitive to temperature (Table 2), while CO_2 concentrations for both optimal growth and for inhibition of rates to half the maximum ($\mathrm{K}\frac{1}{2}_{CO_2}inhib$) decreased with increasing temperature for all rates (Table 2).

3.3 Responses to light

Light intensities affected all physiological rates, with the greatest effect generally being observed at CO_2 concentrations at or above the optimum (Figure 2). Between 50 and 1200 $\mu\mathrm{mol\,photons\,m^{-2}s^{-1}}$, calcification rates doubled, photosynthetic rates tripled and growth rates increased around 36% (Figure 2, Table 3). Both optimum CO_2 and CO_2 concentrations at which rates were half saturated ($\mathrm{K}\frac{1}{2}_{CO_2}sat$) increased slightly with increasing light intensity (Table 3). CO_2 concentrations required to inhibit rates to half of maximum ($\mathrm{K}\frac{1}{2}_{CO_2}inhib$) for calcification and photosynthesis increased with increasing light intensity, while those for growth increased from 50-150 $\mu\mathrm{mol\,photons\,m^{-2}s^{-1}}$ before decreasing with further increases in light (Table 3).

4 Discussion

4.1 Responses to changing carbonate chemistry: CO_2 and H^+

Rates of photosynthesis, calcification and growth in coccolithophores are strongly influenced by CO_2 (Bach et al., 2011; Sett et al., 2014; Zhang et al., 2015). Increasing CO_2 concentrations resulted in enhanced rates up to an optimum level beyond

Biogeosciences Discuss., https://doi.org/10.5194/bg-2018-88
Manuscript under review for journal Biogeosciences
Discussion started: 1 March 2018

which they then declined again. This pattern in growth, photosynthetic carbon fixation and calcification rates has been observed previously for several coccolithophore species (Sett et al., 2014; Bach et al., 2015). The availability of substrate (CO_2 and HCO_3^-) was suggested as the factor influencing the increase in rates on the left side of the optimum, while the proton concentration ($[H^+]$) was the factor most likely driving declines to the right side of the optimum (Bach et al., 2011, 2015).

Of the two species, *E. huxleyi* has a higher CO_2 optimum than *G. oceanica* (Tables 2 and 3, Gafar et al. 2018) for all rates and under most conditions. This could suggest that *E. huxleyi* has a slightly higher substrate requirement than *G. oceanica*. However, considering that *G. oceanica* has both a larger cell size and higher carbon quotas per cell the opposite would be expected (Sett et al., 2014; Bach et al., 2015). An explanation for achieving maximum rates only at higher CO_2 concentrations in *E. huxleyi*, in comparison to *G. oceanica* despite a lower inorganic carbon demand, might be a less efficient or capable carbon uptake/ concentrating mechanism. Alternatively, a decreased sensitivity to high $[H^+]$ in *E. huxleyi*, in comparison to *G. oceanica* (see below), would lead to a shift in the optimum towards higher CO_2 as well and might be a more likely explanation.

Of the three rates, calcification in *E. huxleyi* had both the lowest CO_2 requirement and the highest sensitivity to increasing $[H^+]$ (Tables 3 and 2). This is a pattern previously observed for *G. oceanica* under varying temperature and light conditions (Gafar et al. 2018, See also Table S3). As evidenced by higher $K_{\frac{1}{2}CO_2}inhib$ values for all processes, *E. huxleyi* also appears less sensitive to the inhibiting effects of increasing $[H^+]$ than *G. oceanica* (i.e. $K_{\frac{1}{2}CO_2}inhib$ = 47-250 $\mu mol\,kg^{-1}$ versus 25-99 $\mu mol\,kg^{-1}$ for *G. oceanica* depending on light intensities or $K_{\frac{1}{2}CO_2}inhib$ = 62-250 $\mu mol\,kg^{-1}$ versus 25-130 $\mu mol\,kg^{-1}$ for *G. oceanica* depending on temperature) (Tables 2, 3, S3, Gafar et al. 2018). This also supports earlier results in a model analysis by Bach et al. (2015) where *E. huxleyi* reacted less sensitively to higher CO_2 (and $[H^+]$) than *G. oceanica*.

A lower sensitivity of rates to changes in carbonate chemistry speciation, in particular calcification rates, could be explained by the lower degree of calcification in *E. huxleyi* (PIC:POC ratios 0.24-1.38) when compared to *G. oceanica* (PIC:POC ratios 0.82-2.17) (Sett et al., 2014). Higher rates of calcification result in greater production of intracellular H^+ ($Ca^{2+} + HCO_3^- \rightleftharpoons CaCO_3 + H^+$), potentially decreasing $[CO_3^{2-}]$ in the coccolith producing vesicle and hence the $CaCO_3$ saturation state (Bach et al., 2015). Furthermore, increased $[H^+]$ has been found to result in declines in $[HCO_3^-]$ uptake, the primary carbon source for calcification (Kottmeier et al., 2016).

4.2 Responses to temperature

Temperature was observed to have few modulating effects on CO_2 responses in *E. huxleyi*. Changes in temperature produced little (<11 $\mu mol\,kg^{-1}$) change in CO_2 optima and substrate saturation ($K_{\frac{1}{2}CO_2}sat$) levels, at least within the measured range (Figure 1, Table 2). Similar results were observed for *G. oceanica* (Gafar et al., 2018). This indicates that while overall rates change, carbon uptake mechanisms appear to scale to maintain internal substrate concentrations and thus cellular requirements regardless of temperature conditions.

Biogeosciences Discuss., https://doi.org/10.5194/bg-2018-88
Manuscript under review for journal Biogeosciences
Discussion started: 1 March 2018

In contrast, the inhibition of rates by rising [H^+] i.e. $K_{\frac{1}{2}CO_2}inhib$ was more sensitive to temperature. The CO_2 concentration at which rates were reduced to half the maximum increased with decreasing temperatures (Table 2). These results were also observed for *G. oceanica* which had a lower sensitivity to increasing [H^+] at the lowest tested temperature (Gafar et al., 2018). This also agrees with De Bodt et al. (2010) in which a greater decline in calcification rate was observed with increasing CO_2 at 18°C than at 13°C. These results indicate that, at least some, coccolithophores may be less sensitive to high CO_2 levels at lower temperatures. As a result, both *G. oceanica* and *E. huxleyi* may become more vulnerable to the negative effects of ocean acidification as ocean temperatures increase due to climate change.

4.3 Responses to light

The sensitivity of all rates in *E. huxleyi* to changing carbonate chemistry, in particular increasing [H^+], was clearly modulated by light intensity (Figure 2), agreeing with earlier findings (Zondervan et al., 2002; Feng et al., 2008; Gao et al., 2009; Rokitta and Rost, 2012; Zhang et al., 2015). CO_2 half-saturation ($K_{\frac{1}{2}CO_2}sat$) for all rates were insensitive to increasing light intensities (Table S3). This agrees with results for *G. oceanica* which also displayed little change in CO_2 half-saturation concentrations with increasing light (Table S3). Increasing light intensity induced increases in CO_2 optima in all rates, however these changes were small (<10 $\mu mol\,kg^{-1}$) for calcification and growth rates. This contrasts with *G. oceanica* for which a distinct decrease in optimal CO_2 concentrations for growth rates with increasing light intensities was observed (Table S3). However, *G. oceanica* projections are based on a dataset with only three CO_2 concentrations (~16, 31, 45 $\mu mol\,kg^{-1}$). As such, it is difficult to determine how robust the estimates of CO_2 optima and half-saturation requirements may be for this species (Zhang et al., 2015).

In *E. huxleyi* the relationship between H^+ sensitivity and light intensity was the same for the three rates. Calcification and photosynthetic carbon fixation and growth rates were most sensitive to H^+ at the lowest (50 $\mu mol\,photons\,m^{-2}s^{-1}$) and growth rates were also slightly more sensitive at the highest (1200 $\mu mol\,photons\,m^{-2}s^{-1}$) light intensities (Table 3). This result is in part due to an underestimation of growth rates by the fitting equation under high CO_2 conditions at 50 $\mu mol\,photons\,m^{-2}s^{-1}$ light (Figure 2). However, it may be that sub-optimal light intensities add additional stress to the cells resulting in them having less resources with which to handle the stress of increasing high [H^+]. Hence rates are lower, but also appear more sensitive to changing carbonate chemistry. These findings agree with findings by Rokitta and Rost (2012) where a diploid *E. huxleyi* strain became insensitive to the effects of rising CO_2 (380 vs. 1000 μatm) when light intensities were increased from 50 to 300 $\mu mol\,photons\,m^{-2}s^{-1}$. However, this differs to *G. oceanica* which, with rising light intensities, had no change in sensitivity for calcification rates, a decrease in sensitivity for photosynthesis and an increase in sensitivity for growth rates (Table S3). Again, although this could be indicative for species specific differences in sensitivity, it may also be a result of the low number of CO_2 treatments used in the light data of *G. oceanica* (see Zhang et al. 2015).

Biogeosciences Discuss., https://doi.org/10.5194/bg-2018-88
Manuscript under review for journal Biogeosciences
Discussion started: 1 March 2018

4.4 *E. huxleyi* and *G. oceanica* a niche comparison

In the future ocean CO_2, temperature and light availability are all expected to change (Rost and Riebesell, 2004; IPCC, 2013b). Levels of fCO_2 are expected to reach as high as 985 μatm by the end of the century with concomitant rise in global ocean temperature of up to 4.8°C (RCP8.5 scenario IPCC 2013a, b). Light intensities in the surface ocean are also expected to increase as a result of mixed layer depth shoaling (Rost and Riebesell, 2004). By calculating and comparing growth rates for *E. huxleyi* and *G. oceanica* over a range of environmental conditions, it is possible to differentiate between the fundamental (physiological) niche of a species and its potentially realised niche when in competition with others. For this purpose, light, temperature and CO_2 ranges were restricted to those where both species would be expected to co-occur, i.e. 20-1000 μmol photons $m^{-2}s^{-1}$, 8-30°C and 25-4000 μatm, respectively. The calculated difference in growth rates in response to CO_2 and temperature does not significantly change with light intensity (Figure 3 and 4). It should be noted, however, that light intensity might modify observed growth rate differences for other strains of the same species than used here as they can possess different sensitivities and requirements (i.e. Langer et al. 2009; Müller et al. 2015).

4.4.1 Fundamental niche

Experimentally, *E. huxleyi* has been found to grow in a range of ~6 to 2500 μmol photons $m^{-2}s^{-1}$ with high light resulting in no inhibition of maximum rates in some strains, and up to 20% reduction in others (Balch et al., 1992; van Bleijswijk et al., 1994; Nielsen, 1995; Nanninga and Tyrrell, 1996; van Rijssel and Gieskes, 2002). In contrast, *G. oceanica* is more sensitive in a similar experimental range of ~6-2400 μmol photons $m^{-2}s^{-1}$ with maximum rates inhibited by up to 38% at high light intensities (Larsen, 2012). Light intensities below 6 μmol photons $m^{-2}s^{-1}$ for *E. huxleyi* and *G. oceanica* resulted in no growth for both species (van Bleijswijk et al., 1994; van Rijssel and Gieskes, 2002; Larsen, 2012). So, while *G. oceanica* is more sensitive to high light, the potential upper light limit for growth in both species is beyond naturally occurring maxima. Within this light range both species show a similar increase in projected absolute growth rates of 0-1.57 (d^{-1}) for *E. huxleyi* and 0-1.51 (d^{-1}) for *G. oceanica* (based on figure 4).

E. huxleyi has been successfully cultured at pCO_2 levels between ~20-5600 μatm, while *G. oceanica* has been successfully cultured at pCO_2 levels of ~20-3400 μatm (Sett et al., 2014). Again, the upper tolerance limit for growth in both is not known and well above what is expected for most ocean systems. Responses in projected growth rates with rising CO_2 differ between the two species with *G. oceanica* rates dropping to 50% of maximum at fCO_2 levels above ~1760 μatm while *E. huxleyi* drops to 50% of maximum at ~5950 μatm. In terms of temperature *E. huxleyi* has a broader niche of 3-29°C in comparison to *G. oceanica* at 10-32°C. Within this temperature niche both species again show a similar change in absolute growth rates of 0-1.40 (d^{-1}) for *G. oceanica* and 0-1.43 (d^{-1}) for *E. huxleyi* (based on figure 5).

It should be noted however, that although niche ranges and maximum rates are similar for both species, different requirements ($K\frac{1}{2}sat$) and sensitivities ($K\frac{1}{2}inhib$) will lead to different actual rates at a specific environmental condition. This becomes ev-

ident when examining the temperature, light and CO_2 niches to find a combination of conditions at which growth rate for each species is at its maximum. For *E. huxleyi* maximum growth rates of 1.62 (d^{-1}) are projected at ~970 $\mu mol photons m^{-2} s^{-1}$ light, ~640 μatm CO_2 and 20.2°C. In contrast, the conditions for optimal growth rates of 1.52 (d^{-1}) for *G. oceanica* are achieved at ~500 $\mu mol photons m^{-2} s^{-1}$ light, ~430 μatm CO_2 and 24.4°C. Differences in sensitivity and therefore performance under certain conditions will influence the potentially realised niche of the species. For example, *E. huxleyi* is projected to reach higher growth rates than *G. oceanica* under a broader range of temperature, light and CO_2 conditions (Figures 3, 4 and 5), indicating that this species may be more of a generalist.

4.4.2 Potentially realised niche

Temperature and CO_2 both have substantial effects on the potentially realised niche, of *E. huxleyi* and *G. oceanica* (Figures 4 and 5). In contrast, light intensity has very little effect (Figure 3). *E. huxleyi* appears able to exceed growth rates of *G. oceanica* at temperatures below 22°C under most CO_2 and light conditions (Figures 4 and 5). A similar difference in temperature preferences has also been observed in New Zealand isolates of *Gephyrocapsa oceanica* and *Emiliania huxleyi* with *G. oceanica* and *E. huxleyi* growing between 10-25°C and 5-25°C at optimum temperatures of 22°C and 20°C, respectively (Rhodes et al., 1995). While these results are based on single strain laboratory experiments, there is evidence that such differences in temperature sensitivity may also hold true in the modern ocean. For example, data gathered from multiple phytoplankton monitoring cruises indicate that while both species are found at higher temperatures, *G. oceanica* largely vanishes from the assemblage at temperatures below 13°C (McIntyre and Bé, 1967; Eynaud et al., 1999; Hagino et al., 2005). However, phytoplankton monitoring cruises can be seasonally biased and represent a single point in time.

Another way to relate our niche comparison to today's oceans is through surface sediments. Surface sediment samples represent an integrated signal of the composition of a phytoplankton community over time and can therefore be a more suitable proxy of species dominance in a certain location. Global surface sediment data on *G oceanica* and *E. huxleyi* coccolith abundance indicates that the dominance of these two species is influenced by temperature, particularly in the Pacific Ocean (Figure 6). Globally the data suggests that dominance switches from *E. huxleyi* to *G. oceanica* at temperatures above 25°C which is similar to our projections. It is noted, however, that in the Atlantic Ocean there appears to be a warm water *E. huxleyi* strain outcompeting *G. oceanica* at temperatures above 25 degrees. While both species have a similar upper limit to their fundamental thermal niche (i.e. Rhodes et al. 1995), it would appear that the higher minimum temperature of *G. oceanica*, combined with its greater tolerance for high temperatures, restricts its realised niche to the upper end of the temperature range (Figures 4 and 6).

CO_2 level also influences the relative growth rates of *E. huxleyi* and *G. oceanica*. Under current day levels of ~400 μatm, *E. huxleyi* would dominate at temperatures up to 22°C (Figure 5). However, at higher and lower CO_2 levels, *E. huxleyi* begins to outgrow *G. oceanica* at progressively higher temperatures. At extreme CO_2 levels of 25 and 4000 μatm *G. oceanica* is only projected to reach higher growth rates than *E. huxleyi* at temperatures above 29°C (Figure 5). This is also supported by Rhodes et al. (1995) and Bach et al. (2015) which suggest that *G. oceanica* begin to be inhibited at lower CO_2 (higher H^+)

Biogeosciences Discuss., https://doi.org/10.5194/bg-2018-88
Manuscript under review for journal Biogeosciences
Discussion started: 1 March 2018

than *E. huxleyi*. So, while growth rates in both species are negatively affected by increasing [H^+], *G. oceanica* is more sensitive so its rates decrease relative to *E. huxleyi* for the same change in fCO_2. However, this sensitivity is partially mitigated by increasing temperatures. For example, under RCP scenario 8.5 temperature and CO_2 levels are expected to increase up to 4.8 °C and 985 μatm, respectively. Under higher temperature conditions alone *G. oceanica* would be able to outgrow *E. huxleyi* under a broader range of CO_2 conditions (Figure 5). Meanwhile, under higher CO_2 conditions alone the thermal niche of *G. oceanica* would decrease with this species being dominated by *E. huxleyi* at temperatures up to 26°C. The combined effect of rising temperature and CO_2 allows *G. oceanica* to outgrow *E. huxleyi* under a broader range of CO_2 conditions but a narrower temperature range. As a result, *G. oceanica*' s niche would be expected to decrease under future ocean conditions.

This comparison only considers *E. huxleyi* and *G. oceanica*. However, coccolithophore communities can be made up of dozens of species (McIntyre and Bé, 1967; Winter and Siesser, 1994), all of which are likely to have different preferences for and sensitivities to changes in fCO_2, temperature and light. Shifts in plankton community structure, as a result of different species and group preferences, in response to environmental change have already been observed in the past (Beaugrand et al., 2013; Rivero-Calle et al., 2015), while simulations also suggest shifts in plankton community under future climate conditions (Dutkiewicz et al., 2015). Species and composition shifts in the coccolithophore communities are likely to alter ocean biogeochemistry with implications for ocean-atmosphere CO_2 partitioning.

4.5 Global calcium carbonate production potential

The $CaCO_3$ production potential (CCPP) is based on cellular $CaCO_3$ quotas and growth rates calculated for a given set of temperature, light and carbonate chemistry conditions (see section 2.10). Here we test how this measure for productivity compares to estimated surface ocean $CaCO_3$ content observed by satellite imaging (PIC_s). At this point it is important to remember that CCPP does not account for top-down controls such as grazing or viral attack (Holligan et al., 1993; Wilson et al., 2002; Behrenfeld, 2014), and bottom-up controls such as competition for macro or micro-nutrients (Zondervan, 2007; Browning et al., 2017). Thus, a potential for high $CaCO_3$ production is not necessarily realised when exposed to different top-down and bottom up pressures.

Calculated CCPP of *E. huxleyi* alone (Figure 7) for the global ocean visually reproduces the mid-latitude production belts, however at lower latitudes than satellite PIC estimates. This agrees with the NEMO and OCCAM models of coccolithophore dominance (Sinha et al., 2010) and the chlorophyll a NASA Ocean Biogeochemical Model (NOBM) model for the Southern hemisphere and central North Atlantic provinces (Gregg and Casey, 2007). CCPP also estimates seasonal changes with higher productivity during summer in both hemispheres (see figure 7A and D vs. B and E). This pattern is driven mainly by temperature, which influences the latitudinal location of the bands, and light intensity, which influences whether the northern or southern band of productivity is stronger in a season. Nutrients are an essential, and in the ocean often limiting, requirement for biological productivity (Kattner et al., 2004; Browning et al., 2017). As such it would be expected that nutrients should also be strongly influencing seasonal patterns of PIC production. However, with the starting cell concentrations for the CCPP

calculations chosen here, there was sufficient nitrate to support the projected production in most ocean regions (Figure 7C and F). High temperatures drove relatively low productivity in the equatorial regions in agreement with satellite PIC. Similar low levels of coccolithophores are estimated in Sinha et al. (2010) in the equatorial Pacific and Atlantic with the mixed phytoplankton functional group dominating with or without coccolithophores due to low iron and moderate phosphate concentrations and in Gregg and Casey (2007) for the equatorial Indian and Atlantic provinces. CCPP underestimates production at cold high latitudes, in particular in the Southern Ocean, when compared to the satellite. Similar low levels of coccolithophores have been projected in the Southern Ocean in Gregg and Casey (2007) (very low coccolithophore chlorophyll a), Krumhardt et al. (2017) (growth rates at or close to zero which equates to low to zero CCPP) and Sinha et al. (2010) (high nutrients resulting in coccolithophores being dominated by diatoms). For the Southern Ocean, it has been suggested that satellite PIC concentrations in subantarctic waters are overestimated by a factor of 2-3 while those in Antarctic waters may be even more so (Holligan et al., 2010; Balch et al., 2011; Trull et al., 2018). The fact that three other global estimates, based on different sets of environmental parameters, all estimate very little productivity in the Southern Ocean seems to support this theory. However, there are also specifically cold adapted strains of *Emiliania huxleyi* found at high latitudes which at least partially could explain discrepancies between the mentioned model projections and satellite derived PIC concentrations (see also below).

In Austral winter/Boreal summer CCPP (for *E. huxleyi*) and satellite PIC estimates closely match (R^2=0.73 F=26.78 p<0.01) with low PIC in the South and central South provinces, very low PIC in the equatorial, North Indian and Antarctic provinces and higher PIC in the North central Pacific, North Pacific and North Atlantic provinces (Figure 8A). In Austral summer/Boreal winter CCPP (for *E. huxleyi*) and satellite PIC estimates in individual ocean provinces are also generally of overall good agreement (R^2=0.85 F=50.01 p<0.01). Both CCPP and satellite PIC estimates for Austral summer/Boreal winter are low in all equatorial and North ocean provinces with slightly higher CCPP and satellite PIC production for the North central provinces and higher production in the South and South central provinces (Figure 8B).

Despite having similar PIC patterns, overall PIC estimates can differ significantly between CCPP and PIC_s in some provinces. These provinces can be divided into two groups characterized by either greater or lesser PIC estimates than those observed by satellite (Figure 8). The mid-latitude provinces of central South and central North Pacific and Atlantic and central South Indic in the summer season belong to the former, with higher CCPP than PIC_s. Recently, low phytoplankton biomass in these subtropical gyre systems have been hypothesized to be the result of strong grazing pressure despite high cellular growth rates (Behrenfeld, 2014), lending an explanation of why CCPP is higher than satellite PIC standing stocks. The lower PIC standing stocks estimated from the satellite could also be the result of other phytoplankton functional groups, such as diatoms, taking a comparatively bigger nutrient share (Iglesias-Rodríguez et al., 2002) thereby leaving less for PIC production by coccolithophores.

In contrast, in Austral summer/Boreal winter in the Antarctic and Austral winter/Boreal summer in the North Pacific, CCPP is smaller than satellite PIC estimates (Figure 8). *E. huxleyi*, which our projections are based off, has been found to dominate

assemblages in polar areas, particularly in the southern hemisphere (Okada and Honjo, 1973; Gravalosa et al., 2008; Mohan et al., 2008; Charalampopoulou, 2011). The strains of *E. huxleyi* found here are special cold-adapted ones which can survive at temperatures as low as -1.7°C in the Antarctic (Cubillos et al., 2007) and -0.9°C in the Arctic (Charalampopoulou, 2011)). As our CCPP is based on a temperate coccolithophore strain, lacking the cold adapted ones, our projections underestimate coccolithophore productivity in these areas. Additionally, differences in CCPP and satellite PIC in the Southern Ocean may also be connected to satellite overestimation of PIC at high southern latitudes (see above).

Comparing satellite PIC and CCPP in different oceanic provinces (Figure S1) *E. huxleyi* alone provided the greatest agreement between both. The addition of *G. oceanica* to CCPP calculations negatively affected correlations with satellite PIC. This is counter-intuitive as one would expect increasing correlation of CCPP with satellite PIC as more species are used for the projection of the former. Indeed, estimates based on a combination of *E. huxleyi* and *G. oceanica* in Austral summer/Boreal winter were similar to those for *E. huxleyi* alone. However, in Austral winter/Boreal summer estimates based on a combination of *E. huxleyi* and *G. oceanica* resulted in much lower agreement between CCPP and satellite PIC when compared to *E. huxleyi* alone. This difference is driven by greatly increased CCPP estimates in the central North Pacific and Atlantic, combined with greatly decreased CCPP estimates in the North Pacific and Atlantic, relative to the *E. huxleyi* alone fit. Being a warm adapted species including *G. oceanica* would result in more productivity in the sub-tropical zones. However, these zones are also regions of potentially significant top-down control (see above for details). Meanwhile the North Pacific and Atlantic are likely dominated by cold-adapted species (see above for details), so including the warm-adapted *G. oceanica* in CCPP calculations would further reduce estimates in these regions. As a result, the inclusion of *G. oceanica* does not assist in making global estimates of coccolithophore PIC production.

5 Conclusions

Our analysis of the projected combination of increased temperature and CO_2 on potential success, in terms of growth rates, suggests that *E. huxleyi* will benefit over *G. oceanica*. Due to a greater sensitivity to CO_2, *G. oceanica*'s niche will likely contract to regions of higher temperature under future ocean conditions. In general, changes in community composition can influence community level carbon production and sequestration by coccolithophores. Such changes could have significant implications for climate feedback mechanisms, one being the effects on the relative strength of the organic and inorganic carbon pumps, especially in coccolithophore dominated ecosystems. Temperature and light were found to be important factors driving projections of $CaCO_3$ production potential (CCPP) on a global scale. Comparison of satellite derived inorganic carbon versus estimated inorganic carbon suggests that *E. huxleyi* CCPP is a good proxy for coccolithophore community production in most biogeographical provinces. However, results indicate that data on the responses of polar species and strains, to environmental change, may be required to improve estimates in the high-latitudes, while the effects of top-down controls might be needed to improve estimates in the mid-latitudes.

Data availability. All data used for the calculation of model fits and coefficients for *Emiliania huxleyi* can be found in the supplementary material for this paper. Fit coefficients used for calculation of *Gephyrocapsa oceanica* niches can be found in Gafar et al. (2018) (DOI: 10.3389/fmars.2017.00433). Third party data sets used for calculation of global calcium carbonate production potential are detailed in Sect. 4.5

.

Author contributions. Conceived and designed the experiments: KS NG.
Performed the experiments: NG.
Analysed the data: NG KS.
Wrote the paper: NG KS.

Competing interests. The authors declare that they have no conflict of interest.

Acknowledgements. This study was funded by the Australian Research Council (ARC) FT120100384 awarded to KGS and DP150102092 awarded to KGS. We also thank Dr. Matheus Carvalho for analysing particulate carbon samples.

References

Andruleit, H. and Rogalla, U.: Coccolithophores in surface sediments of the Arabian Sea in relation to environmental gradients in surface waters, Marine Geology, 186, 505–526, https://doi.org/10.1016/S0025-3227(02)00312-2, 2002.

Bach, L. T., Riebesell, U., and Schulz, K. G.: Distinguishing between the effects of ocean acidification and ocean carbonation in the coccolithophore *Emiliania huxleyi*, Limnology and Oceanography, 56, 2040–2050, https://doi.org/10.4319/lo.2011.56.6.2040, 2011.

Bach, L. T., MacKinder, L. C. M., Schulz, K. G., Wheeler, G., Schroeder, D. C., Brownlee, C., and Riebesell, U.: Dissecting the impact of CO_2 and pH on the mechanisms of photosynthesis and calcification in the coccolithophore *Emiliania huxleyi*, New Phytologist, 199, 121–134, https://doi.org/10.1111/nph.12225, 2013.

Bach, L. T., Riebesell, U., Gutowska, M. A., Federwisch, L., and Schulz, K. G.: A unifying concept of coccolithophore sensitivity to changing carbonate chemistry embedded in an ecological framework, Progress in Oceanography, 135, 125–138, https://doi.org/10.1016/j.pocean.2015.04.012, 2015.

Balch, W., Drapeau, D., Bowler, B., Lyczskowski, E., Booth, E., and Alley, D.: The contribution of coccolithophores to the optical and inorganic carbon budgets during the Southern Ocean Gas Exchange Experiment: New evidence in support of the ''Great Calcite Belt" hypothesis, Journal of Geophysical Research: Oceans, 116, C00F06, https://doi.org/10.1029/2011JC006941, 2011.

Balch, W. M., Holligan, P. M., and Kilpatrick, K. A.: Calcification, photosynthesis and growth of the bloom-forming coccolithophore, *Emiliania huxleyi*, Continental Shelf Research, 12, 1353–1374, https://doi.org/10.1016/0278-4343(92)90059-S, 1992.

Baumann, K.-H., Andruleit, H., and Samtleben, C.: Coccolithophores in the Nordic Seas: Comparison of living communities with surface sediment assemblages, Deep Sea Research Part II: Topical Studies in Oceanography, 47, 1743–1772, https://doi.org/10.1016/S0967-0645(00)00005-9, http://www.sciencedirect.com/science/article/pii/S0967064500000059, 2000.

Beaugrand, G., McQuatters-Gollop, A., Edwards, M., and Goberville, E.: Long-term responses of North Atlantic calcifying plankton to climate change, Nature Climate Change, 3, 263–267, https://doi.org/10.1038/nclimate1753, 2013.

Behrenfeld, M. J.: Climate-mediated dance of the plankton, Nature Climate Change, 4, 880–887, https://doi.org/10.1038/NCLIMATE2349, 2014.

Bockmon, E. E. and Dickson, A. G.: A seawater filtration method suitable for total dissolved inorganic carbon and pH analyses, Limnology and Oceanography: Methods, 12, 191–195, https://doi.org/10.4319/lom.2014.12.191, 2014.

Boeckel, B. and Baumann, K.-H.: Vertical and lateral variations in coccolithophore community structure across the subtropical frontal zone in the South Atlantic Ocean, Marine Micropaleontology, 67, 255–273, https://doi.org/10.1016/j.marmicro.2008.01.014, 2008.

Boeckel, B., Baumann, K.-H., Henrich, R., and Kinkel, H.: Coccolith distribution patterns in South Atlantic and Southern Ocean surface sediments in relation to environmental gradients, Deep Sea Research Part I: Oceanographic Research Papers, 53, 1073–1099, https://doi.org/10.1016/j.dsr.2005.11.006, http://www.sciencedirect.com/science/article/pii/S0967063706000045, 2006.

Bopp, L., Monfray, P., Aumont, O., Dufresne, J.-L., Le Treut, H., Madec, G., Terray, L., and Orr, J. C.: Potential impact of climate change on marine export production, Global Biogeochemical Cycles, 15, 81–99, https://doi.org/10.1029/1999GB001256, 2001.

Boyer, T. P., Antonov, J. I., Baranova, O. K., Coleman, C., Garcia, H. E., Grodsky, A., Johnson, D. R., Locarnini, R. A., Mishonov, A. V., and O'Brien, T. D.: World Ocean Database 2013, NOAA Atlas NESDIS 72, National Oceanographic Data Center, Silver Spring, MD, USA, https://doi.org/10.2481/dsj.WDS-041, 2013.

Broecker, W. and Clark, E.: Ratio of coccolith $CaCO_3$ to foraminifera $CaCO_3$ in late Holocene deep sea sediments, Paleoceanography, 24, PA3205, https://doi.org/10.1029/2009PA001731, 2009.

Browning, T. J., Achterberg, E. P., Rapp, I., Engel, A., Bertrand, E. M., Tagliabue, A., and Moore, C. M.: Nutrient co-limitation at the boundary of an oceanic gyre, Nature, 551, 242–246, https://doi.org/10.1038/nature24063, 2017.

Caldeira, K. and Wickett, M. E.: Ocean model predictions of chemistry changes from carbon dioxide emissions to the atmosphere and ocean, Journal of Geophysical Research, 110, C09S04, https://doi.org/10.1029/2004jc002671, 2005.

Charalampopoulou, A.: Coccolithophores in high latitude and polar regions: Relationships between community composition, calcification and environmental factors, Doctor of philosophy, School of Ocean and Earth Science, Southampton, 2011.

Chen, M. and Shieh, K.: Recent nannofossil assemblages in sediments from Sunda Shelf to abyssal plain, South China Sea, Proceedings of the National Science Council (ROC), Part A, 6, 250–285, 1982.

Cubillos, J. C., Wright, S. W., Nash, G., De Salas, M. F., Griffiths, B., Tilbrook, B., Poisson, A., and Hallegraeff, G. M.: Calcification morphotypes of the coccolithophorid *Emiliania huxleyi* in the Southern Ocean: Changes in 2001 to 2006 compared to historical data, Marine Ecology Progress Series, 348, 47–54, https://doi.org/10.3354/meps07058, 2007.

De Bodt, C., Van Oostende, N., Harlay, J., Sabbe, K., and Chou, L.: Individual and interacting effects of pCO_2 and temperature on *Emiliania huxleyi* calcification: Study of the calcite production, the coccolith morphology and the coccosphere size, Biogeosciences, 7, 1401–1412, https://doi.org/10.5194/bg-7-1401-2010, 2010.

de Boyer Montégut, C., Madec, G., Fischer, A. S., Lazar, A., and Iudicone, D.: Mixed layer depth over the global ocean: An examination of profile data and a profile-based climatology, Journal of Geophysical Research: Oceans, 109, https://doi.org/10.1029/2004JC002378, 2004.

Dickson, A. G.: Standards for ocean measurements, Oceanography, 23, 34–47, https://doi.org/10.5670/oceanog.2010.22, 2010.

Dickson, A. G., Wesolowski, D. J., Palmer, D. A., and Mesmer, R. E.: Dissociation constant of bisulfate ion in aqueous sodium chloride solutions to 250°C, Journal of Physical Chemistry, 94, 7978–7985, https://doi.org/10.1021/j100383a042, 1990.

Dickson, A. G., Sabine, C. L., and Christian, J. R.: Guide to best practices for ocean CO_2 measurements, PICES Special Publication, North Pacific Marine Science Organization, Sidney, British Columbia, 2007.

Doney, S. C., Fabry, V. J., Feely, R. A., and Kleypas, J. A.: Ocean acidification: The other CO_2 problem, Annual Review of Marine Science, 1, 169–192, https://doi.org/10.1146/annurev.marine.010908.163834, 2009.

Dutkiewicz, S., Morris, J. J., Follows, M. J., Scott, J., Levitan, O., Dyhrman, S. T., and Berman-Frank, I.: Impact of ocean acidification on the structure of future phytoplankton communities, Nature Climate Change, 5, 1002–1006, https://doi.org/10.1038/nclimate2722, 2015.

Endo, H., Yoshimura, T., Kataoka, T., and Suzuki, K.: Effects of CO_2 and iron availability on phytoplankton and eubacterial community compositions in the northwest subarctic Pacific, Journal of Experimental Marine Biology and Ecology, 439, 160–175, https://doi.org/10.1016/j.jembe.2012.11.003, 2013.

Engel, A., Zondervan, I., Aerts, K., Beaufort, L., Benthien, A., Chou, L., Delille, B., Gattuso, J.-P., Harlay, J., Heemann, C., Hoffmann, L., Jacquet, S., Nejstgaard, J., Pizay, M.-D., Rochelle-Newall, E., Schneider, U., Terbrueggen, A., and Riebesell, U.: Testing the direct effect of CO_2 concentration on a bloom of the coccolithophorid *Emiliania huxleyi* in mesocosm experiments, Limnology and Oceanography, 50, 493–507, https://doi.org/10.4319/lo.2005.50.2.0493, 2005.

Eynaud, F., Giraudeau, J., Pichon, J.-J., and Pudsey, C. J.: Sea-surface distribution of coccolithophores, diatoms, silicoflagellates and dinoflagellates in the South Atlantic Ocean during the late austral summer 1995, Deep-sea research. Part I: Oceanographic Research Papers, 46, 451–482, https://doi.org/10.1016/S0967-0637(98)00079-X, 1999.

Feng, Y., Warner, M. E., Zhang, Y., Sun, J., Fu, F.-X., Rose, J. M., and Hutchins, D. A.: Interactive effects of increased pCO_2, temperature and irradiance on the marine coccolithophore *Emiliania huxleyi* (Prymnesiophyceae), European Journal of Phycology, 43, 87–98, https://doi.org/10.1080/09670260701664674, 2008.

Feng, Y., Hare, C. E., Rose, J., Handy, S. M., DiTullio, G. R., Lee, P. A., Smith Jr, W. O., Peloquin, J., Tozzi, S., Sun, J., Zhang, Y., Dunbar, R. B., Long, M. C., Sohst, B., Lohan, M., and Hutchins, D. A.: Interactive effects of iron, irradiance and CO_2 on Ross Sea phytoplankton, Deep Sea Research Part I: Oceanographic Research Papers, 57, 368–383, https://doi.org/10.1016/j.dsr.2009.10.013, 2010.

Fernando, A. G. S., Peleo-Alampay, A. M., and Wiesner, M. G.: Calcareous nannofossils in surface sediments of the eastern and western South China Sea, Marine Micropaleontology, 66, 1–26, https://doi.org/10.1016/j.marmicro.2007.07.003, 2007.

Gafar, N. A., Eyre, B. D., and Schulz, K. G.: A conceptual model for projecting coccolithophorid growth, calcification and photosynthetic carbon fixation rates in response to global ocean change, Frontiers in Marine Science, 4, 1–18, https://doi.org/10.3389/fmars.2017.00433, 2018.

Gao, K., Ruan, Z., Villafane, V. E., Gattuso, J.-P., and Helbling, E. W.: Ocean acidification exacerbates the effect of UV radiation on the calcifying phytoplankter *Emiliania huxleyi*, Limnology and Oceanography, 54, 1855–1862, https://doi.org/10.4319/lo.2009.54.6.1855, 2009.

Gravalosa, J. M., Flores, J.-A., Sierro, F. J., and Gersonde, R.: Sea surface distribution of coccolithophores in the eastern Pacific sector of the Southern Ocean (Bellingshausen and Amundsen Seas) during the late austral summer of 2001, Marine Micropaleontology, 69, 16–25, https://doi.org/10.1016/j.marmicro.2007.11.006, 2008.

Gregg, W. W. and Casey, N. W.: Modeling coccolithophores in the global oceans, Deep Sea Research Part II: Topical Studies in Oceanography, 54, 447–477, https://doi.org/10.1016/j.dsr2.2006.12.007, http://www.sciencedirect.com/science/article/pii/S0967064507000318, 2007.

Guillard, R. R. L.: Culture of phytoplankton for feeding marine invertebrates, in: Culture of Marine Invertebrate Animals, edited by Smith, W. L. and Chanley, M. H., pp. 26–60, Plenum Press, New York, USA, 1975.

Hagino, K., Okada, H., and Matsuoka, H.: Coccolithophore assemblages and morphotypes of *Emiliania huxleyi* in the boundary zone between the cold Oyashio and warm Kuroshio currents off the coast of Japan, Marine Micropaleontology, 55, 19–47, https://doi.org/10.1016/j.marmicro.2005.02.002, http://www.sciencedirect.com/science/article/pii/S0377839805000149, 2005.

Helm, D., Cook, S., Cubillos, J., McMinn, A., and Hallegraeff, G. M.: Growth, photosynthesis and temperature tolerance of eight Southern Ocean strains of the coccolithophorid *Emiliania huxleyi*, Masters thesis, Institute of Antarctic and Southern Ocean Studies, 2007.

Holligan, P. M., Fernández, E., Aiken, J., Balch, W. M., Boyd, P., Burkill, P. H., Finch, M., Groom, S. B., Malin, G., Muller, K., Purdie, D. A., Robinson, C., Trees, C. C., Turner, S. M., and van der Wal, P.: A biogeochemical study of the coccolithophore,*Emiliania huxleyi*, in the North Atlantic, Global Biogeochemical Cycles, 7, 879–900, https://doi.org/10.1029/93GB01731, 1993.

Holligan, P. M., Charalampopoulou, A., and Hutson, R.: Seasonal distributions of the coccolithophore, *Emiliania huxleyi*, and of particulate inorganic carbon in surface waters of the Scotia Sea, Journal of Marine Systems, 82, 195–205, https://doi.org/10.1016/j.jmarsys.2010.05.007, 2010.

Hutchinson, G.: Concluding remarks, Cold Spring Harbor Symposia on Quantitative Biology, 22, 415–427, 1957.

Iglesias-Rodríguez, M. D., Brown, C. W., Doney, S. C., Kleypas, J., Kolber, D., Kolber, Z., Hayes, P. K., and Falkowski, P. G.: Representing key phytoplankton functional groups in ocean carbon cycle models: Coccolithophorids, Global Biogeochemical Cycles, 16, https://doi.org/10.1029/2001GB001454, 2002.

IPCC: Climate Change 2013: The Physical Science Basis. Contribution of Working Group I to the Fifth Assessment Report of the Intergovernmental Panel on Climate Change, Cambridge University Press, Cambridge, United Kingdom and New York, NY, USA, 2013a.

IPCC: Summary for policy makers, in: Climate Change 2013: The Physical Science Basis. Contribution of Working Group I to the Fifth Assessment Report of the Intergovernmental Panel on Climate Change, edited by Stocker, T. F., Qin, D., Plattner, G.-K., Tignor, M., Allen, S. K., Boschung, J., Nauels, A., Xia, Y., V., B., and Midgley, P. M., pp. 1–27, Cambridge University Press, Cambridge, United Kingdom and New York, NY, USA, 2013b.

Kattner, G., Thomas, D. N., Haas, C., Kennedy, H., and Dieckmann, G. S.: Surface ice and gap layers in Antarctic sea ice: Highly productive habitats, Marine Ecology Progress Series, 277, 1–12, https://doi.org/10.3354/meps277001, http://www.int-res.com/articles/meps2004/277/m277p001.pdf, 2004.

Kester, D. R., Duedall, I. W., Connors, D. N., and Pytkowicz, R. M.: Preparation of artificial seawater, Limnology and Oceanography, 12, 176–179, https://doi.org/10.4319/lo.1967.12.1.0176, 1967.

Knappertsbusch, M.: Geographic distribution of living and Holocene coccolithophores in the Mediterranean Sea, Marine Micropaleontology, 21, 219–247, https://doi.org/10.1016/0377-8398(93)90016-Q, 1993.

Kottmeier, D. M., Rokitta, S. D., and Rost, B.: Acidification, not carbonation, is the major regulator of carbon fluxes in the coccolithophore *Emiliania huxleyi*, New Phytologist, 211, 126–137, https://doi.org/10.1111/nph.13885, 2016.

Krumhardt, K. M., Lovenduski, N. S., Iglesias-Rodriguez, M. D., and Kleypas, J. A.: Coccolithophore growth and calcification in a changing ocean, Progress in Oceanography, 159, 276–295, https://doi.org/10.1016/j.pocean.2017.10.007, 2017.

Langer, G., Nehrke, G., Probert, I., Ly, J., and Ziveri, P.: Strain-specific responses of *Emiliania huxleyi* to changing seawater carbonate chemistry, Biogeosciences Discussions, 6, 4361–4383, https://doi.org/10.5194/bg-6-2637-2009, 2009.

Larsen, S. H.: Dimethylsulphoniopropionate (DMSP) production of *Gephyrocapsa oceanica* in response to environmental forcing, Doctor of philosophy, School of Biological Sciences, Melbourne, https://doi.org/10.4225/03/58a24e0331904, 2012.

Lefebvre, S. C., Benner, I., Stillman, J. H., Parker, A. E., Drake, M. K., Rossignol, P. E., Okimura, K. M., Tomoko, K., and Carpenter, E. J.: Nitrogen source and pCO_2 synergistically affect carbon allocation, growth and morphology of the coccolithophore *Emiliania huxleyi*: Potential implications of ocean acidification for the carbon cycle, Global Change Biology, 18, 493–503, https://doi.org/10.1111/j.1365-2486.2011.02575.x, 2012.

Leibold, M. A.: The niche concept revisited: Mechanistic models and community context, Ecology, 76, 1371–1382, https://doi.org/10.1111/j.1529-8817.2005.00152.x, 1995.

Lewis, E., Wallace, D., and Allison, L. J.: Program developed for CO_2 system calculations, Carbon Dioxide Information Analysis Center, managed by Lockheed Martin Energy Research Corporation for the US Department of Energy Tennessee, Oak Ridge, https://doi.org/10.3334/CDIAC/otg.CO2SYS_DOS_CDIAC105, 1998.

Longhurst, A. R.: Ecological geography of the sea, Ecological Geography of the Sea Series, Elsevier Science, London, UK, 2 edn., 2007.

Lueker, T. J., Dickson, A. G., and Keeling, C. D.: Ocean pCO_2 calculated from dissolved inorganic carbon, alkalinity, and equations for K_1 and K_2: Validation based on laboratory measurements of CO_2 in gas and seawater at equilibrium, Marine Chemistry, 70, 105–119, https://doi.org/10.1016/S0304-4203(00)00022-0, 2000.

McIntyre, A. and Bé, A. W. H.: Modern Coccolithophoridae of Atlantic Ocean -I. Placoliths and cyrtoliths, Deep-Sea Research and Oceanographic Abstracts, 14, 561–597, https://doi.org/10.1016/0011-7471(67)90065-4, 1967.

Mohan, R., Mergulhao, L. P., Guptha, M. V. S., Rajakumar, A., Thamban, M., AnilKumar, N., Sudhakar, M., and Ravindra, R.: Ecology of coccolithophores in the Indian sector of the Southern Ocean, Marine Micropaleontology, 67, 30–45, https://doi.org/10.1016/j.marmicro.2007.08.005, 2008.

Moheimani, N. R. and Borowitzka, M. A.: Increased CO_2 and the effect of pH on growth and calcification of *Pleurochrysis carterae* and *Emiliania huxleyi* (Haptophyta) in semicontinuous cultures, Applied microbiology and biotechnology, 90, 1399–1407, https://doi.org/10.1007/s00253-011-3174-x, 2011.

Müller, M. N., Trull, T. W., and Hallegraeff, G. M.: Differing responses of three Southern Ocean *Emiliania huxleyi* ecotypes to changing seawater carbonate chemistry, Mar. Ecol.-Prog. Ser, 531, 81–90, https://doi.org/10.3354/meps11309, 2015.

Nanninga, H. and Tyrrell, T.: Importance of light for the formation of algal blooms by *Emiliania huxleyi*, Marine ecology progress series. Oldendorf, 136, 195–203, https://doi.org/10.3354/meps136195, 1996.

NASA Goddard Space Flight Center, Ocean Ecology Laboratory, O. B. P. G.: Moderate-resolution Imaging Spectroradiometer (MODIS) Aqua Particulate Inorganic Carbon Data; 2014 Reprocessing, NASA OB.DAAC, Greenbelt, MD, USA, https://doi.org/doi:10.5067/AQUA/MODIS/L3B/PIC/2014, accessed 2/11/2017, 2014a.

NASA Goddard Space Flight Center, Ocean Ecology Laboratory, O. B. P. G.: Moderate-resolution Imaging Spectroradiometer (MODIS) Aqua Photosynthetically Available Radiation Data; 2014 Reprocessing, NASA OB.DAAC, Greenbelt, MD, USA, https://doi.org/10.5067/AQUA/MODIS/L3M/PAR/2014, accessed 30/11/2017, 2014b.

Nielsen, M. V.: Photosynthetic characteristics of the coccolithophorid *Emiliania huxleyi* (Prymnesiophyceae) exposed to elevated concentrations of dissolved inorganic carbon, Journal of Phycology, 31, 715–719, https://doi.org/10.1111/j.0022-3646.1995.00715.x, 1995.

Okada, H. and Honjo, S.: Distribution of coccolithophorids in the North and Equatorial Pacific Ocean: Quantitative data on samples collected during Leg 30, Oshoro-Maru, 1968 and Leg HK69-4, Hakuho-Maru, 1969, Report WHOI-73-81, Woods Hole Oceanographic Institution, Woods hole, Falmouth, unpublished manuscript, 1973.

Orr, J. C., Fabry, V. J., Aumont, O., Bopp, L., Doney, S. C., Feely, R. A., Gnanadesikan, A., Gruber, N., Ishida, A., Joos, F., Key, R. M., Lindsay, K., Maier-Reimer, E., Matear, R., Monfray, P., Mouchet, A., Najjar, R. G., Plattner, G.-K., Rodgers, K. B., Sabine, C. L., Sarmiento, J. L., Schlitzer, R., Slater, R. D., Totterdell, I. J., Weirig, M.-F., Yamanaka, Y., and Yool, A.: Anthropogenic ocean acidification over the twenty-first century and its impact on calcifying organisms, Nature, 437, 681–686, https://doi.org/10.1038/nature04095, 2005.

Paasche, E.: Roles of nitrogen and phosphorus in coccolith formation in *Emiliania huxleyi* (Prymnesiophyceae), European Journal of Phycology, 33, 33–42, https://doi.org/10.1080/09670269810001736513, 1998.

Pascal, D.: GMIS - MERIS Monthly climatology sea surface diffuse attenuation coefficient at 490nm (9km) in m^{-1}, European Commission, Joint Research Centre (JRC), accessed 2/11/2017, 2013.

Patil, S. M., Mohan, R., Shetye, S., Gazi, S., and Jafar, S.: Morphological variability of *Emiliania huxleyi* in the Indian sector of the Southern Ocean during the austral summer of 2010, Marine Micropaleontology, 107, 44–58, https://doi.org/10.1016/j.marmicro.2014.01.005, http://www.sciencedirect.com/science/article/pii/S0377839814000085, 2014.

Poulton, A. J., Adey, T. R., Balch, W. M., and Holligan, P. M.: Relating coccolithophore calcification rates to phytoplankton community dynamics: Regional differences and implications for carbon export, Deep Sea Research Part II: Topical Studies in Oceanography, 54, 538–557, https://doi.org/10.1016/j.dsr2.2006.12.003, 2007.

Poulton, A. J., Charalampopoulou, A., Young, J. R., Tarran, G. A., Lucas, M. I., and Quartly, G. D.: Coccolithophore dynamics in non-bloom conditions during late summer in the central Iceland Basin (July-August 2007), Limnology and Oceanography, 55, 1601–1613, https://doi.org/10.4319/lo.2010.55.4.1601, 2010.

Powles, S. B.: Photoinhibition of photosynthesis induced by visible light, Annual Review of Plant Physiology, 35, 15–44, https://doi.org/10.1146/annurev.pp.35.060184.000311, 1984.

Raven, J. A. and Crawfurd, K.: Environmental controls on coccolithophore calcification, Marine Ecology Progress Series, 470, 137–166, https://doi.org/10.3354/meps09993, 2012.

Rhodes, L. L., Peake, B. M., MacKenzie, A. L., and Marwick, S.: Coccolithophores *Gephyrocapsa oceanica* and *Emiliania huxleyi* (Prymnesiophyceae=Haptophyceae) in New Zealand's coastal waters: Characteristics of blooms and growth in laboratory culture, New Zealand Journal of Marine and Freshwater Research, 29, 345–357, https://doi.org/10.1080/00288330.1995.9516669, 1995.

Riebesell, U., Zondervan, I., Rost, B., Tortell, P. D., Zeebe, R. E., and Morel, F. M. M.: Reduced calcification of marine plankton in response to increased atmospheric CO_2, Nature, 407, 364–367, https://doi.org/10.1038/35030078, 2000.

Rivero-Calle, S., Gnanadesikan, A., Del Castillo, C. E., Balch, W. M., and Guikema, S. D.: Multidecadal increase in North Atlantic coccolithophores and the potential role of rising CO_2, Science, 350, 1533–1537, https://doi.org/10.1126/science.aaa8026, 2015.

Rokitta, S. D. and Rost, B.: Effects of CO_2 and their modulation by light in the life-cycle stages of the coccolithophore *Emiliania huxleyi*, Limnology and Oceanography, 57, 607–618, https://doi.org/10.4319/lo.2012.57.2.0607, 2012.

Rost, B. and Riebesell, U.: Coccolithophores and the biological pump: Responses to environmental changes, in: Coccolithophores: From molecular processes to global impacts, edited by Thierstein, H. R. and Young, J. R., book section 5, pp. 99–125, Springer, Berlin, Heidelberg, https://doi.org/10.1007/978-3-662-06278-4_5, 2004.

Roth, P. H. and Coulbourn, W. T.: Floral and solution patterns of coccoliths in surface sediments of the North Pacific, Marine Micropaleontology, 7, 1–52, https://doi.org/10.1016/0377-8398(82)90014-7, 1982.

Saavedra-Pellitero, M., Baumann, K.-H., Flores, J.-A., and Gersonde, R.: Biogeographic distribution of living coccolithophores in the Pacific Sector of the Southern Ocean, Marine Micropaleontology, 109, 1–20, https://doi.org/10.1016/j.marmicro.2014.03.003, 2014.

Sabine, C. L., Feely, R. A., Gruber, N., Key, R. M., Lee, K., Bullister, J. L., Wanninkhof, R., Wong, C. S. l., Wallace, D. W. R., and Tilbrook, B.: The oceanic sink for anthropogenic CO_2, science, 305, 367–371, https://doi.org/10.1126/science.1097403, 2004.

Samtleben, C. and Schroder, A.: Living coccolithophore communities in the Norwegian-Greenland Sea and their record in sediments, Marine Micropaleontology, 19, 333–354, https://doi.org/10.1016/0377-8398(92)90037-K, 1992.

Schneider, U.: Influence of carbonate chemistry and light intensity on natural phytoplankton assemblages with emphasis on species composition, Doctor of philosophy, Biology/Chemistry, 2004.

Schulz, K. G., Barcelos e Ramos, J., Zeebe, R. E., and Riebesell, U.: CO_2 perturbation experiments: Similarities and differences between dissolved inorganic carbon and total alkalinity manipulations, Biogeosciences, 6, 2145–2153, https://doi.org/10.5194/bgd-6-4441-2009, 2009.

Schulz, K. G., Bach, L. T., Bellerby, R. G., Bermudez, R., B´udenbender, J., Boxhammer, T., Czerny, J., Engel, A., Ludwig, A., and Meyerh´ofer, M.: Phytoplankton blooms at increasing levels of atmospheric carbon dioxide: Experimental evidence for negative effects on prymnesiophytes and positive on small picoeukaryotes, Frontiers in Marine Science, 4, 1–18, https://doi.org/10.3389/fmars.2017.00064., 2017.

Sett, S., Bach, L. T., Schulz, K. G., Koch-Klavsen, S., Lebrato, M., and Riebesell, U.: Temperature modulates coccolithophorid sensitivity of growth, photosynthesis and calcification to increasing seawater pCO_2, PloS one, 9, e88 308, https://doi.org/10.1371/journal.pone.0088308, 2014.

Sharp, J. H.: Improved analysis for "particulate" organic carbon and nitrogen from seawater, Limnology and Oceanography, 19, 984–989, https://doi.org/10.4319/lo.1974.19.6.0984, 1974.

Sinha, B., Buitenhuis, E. T., Le Quéré, C., and Anderson, T. R.: Comparison of the emergent behavior of a complex ecosystem model in two ocean general circulation models, Progress in Oceanography, 84, 204–224, https://doi.org/10.1016/j.pocean.2009.10.003, 2010.

Takahashi, T., Sutherland, S. C., Chipman, D. W., Goddard, J. G., Ho, C., Newberger, T., Sweeney, C., and Munro, D.: Climatological distributions of pH, pCO_2, total CO_2, alkalinity, and $CaCO_3$ saturation in the global surface ocean, and temporal changes at selected locations, Marine Chemistry, 164, 95–125, https://doi.org/10.1016/j.marchem.2014.06.004, 2014.

Trull, T. W., Passmore, A., Davies, D. M., Smit, T., Berry, K., and Tilbrook, B.: Distribution of planktonic biogenic carbonate organisms in the Southern Ocean south of Australia: a baseline for ocean acidification impact assessment, Biogeosciences, 15, 31–49, 2018.

Uppström, L. R.: The boron/chlorinity ratio of deep-sea water from the Pacific Ocean, Deep Sea Research and Oceanographic Abstracts, 21, 161–162, https://doi.org/10.1016/0011-7471(74)90074-6, 1974.

van Bleijswijk, J. D. L., Kempers, R. S., and Velhuis, M. J.: Cell and growth characteristics of types A and B of *Emiliania huxleyi* (Prymnesiophyceae) as determined by flow cytometry and chemical analysis, Journal of Phycology, 30, 230–241, https://doi.org/10.1111/j.0022-3646.1994.00230.x, 1994.

van Rijssel, M. and Gieskes, W. W. C.: Temperature, light, and the dimethylsulfoniopropionate (DMSP) content of *Emiliania huxleyi* (Prymnesiophyceae), Journal of Sea Research, 48, 17–27, https://doi.org/10.1016/S1385-1101(02)00134-X, 2002.

Wilson, W. H., Tarran, G. A., Schroeder, D., Cox, M., Oke, J., and Malin, G.: Isolation of viruses responsible for the demise of an *Emiliania huxleyi* bloom in the English Channel, Journal of the Marine Biological Association of the United Kingdom, 82, 369–377, https://doi.org/10.1017/S002531540200560X, 2002.

Winter, A. and Siesser, W. G.: Atlas of living coccolithophores, in: Coccolithophores, edited by Winter, A. and Siesser, W. G., vol. 13, book section 7, pp. 107–159, Cambridge University Press, Cambridge, United Kingdom, 1994.

Zhang, Y., Klapper, R., Lohbeck, K. T., Bach, L. T., Schulz, K. G., Reusch, T. B. H., and Riebesell, U.: Between-and within-population variations in thermal reaction norms of the coccolithophore *Emiliania huxleyi*, Limnology and oceanography, 59, 1570–1580, https://doi.org/10.4319/lo.2014.59.5.1570, 2014.

Zhang, Y., Bach, L. T., Schulz, K. G., and Riebesell, U.: The modulating influence of light intensity on the response of the coccolithophore *Gephyrocapsa oceanica* to ocean acidification, Limnology and Oceanography, 60, 2145–2157, https://doi.org/10.1002/lno.10161, 2015.

Zondervan, I.: The effects of light, macronutrients, trace metals and CO_2 on the production of calcium carbonate and organic carbon in coccolithophores - A review, Deep Sea Research Part II: Topical Studies in Oceanography, 54, 521–537, https://doi.org/10.1016/j.dsr2.2006.12.004, 2007.

Zondervan, I., Rost, B., and Riebesell, U.: Effect of CO_2 concentration on the PIC/POC ratio in the coccolithophore *Emiliania huxleyi* grown under light-limiting conditions and different daylengths, Journal of Experimental Marine Biology and Ecology, 272, 55–70, https://doi.org/10.1016/S0022-0981(02)00037-0, 2002.

Zurell, D., Thuiller, W., Pagel, J., Cabral, J. S., Münkemüller, T., Gravel, D., Dullinger, S., Normand, S., Schiffers, K. H., and Moore, K. A.: Benchmarking novel approaches for modelling species range dynamics, Global change biology, 22, 2651–2664, https://doi.org/10.1111/gcb.13251, 2016.

Tables and Figures

Biogeosciences Discuss., https://doi.org/10.5194/bg-2018-88
Manuscript under review for journal Biogeosciences
Discussion started: 1 March 2018

Table 1. Fit coefficients (k_1 to k_6), R^2, F-values, degrees of freedom and p-values obtained for calcification (pg C cell^{-1} d^{-1}), photosynthetic carbon fixation (pg C cell^{-1} d^{-1}) and growth rates (d^{-1}) from Eq. (2) fitted to data from this study and Sett et al. (2014). For calcification and photosynthetic carbon fixation rates the unit for v = pg C cell^{-1} day^{-1} while for growth rates the unit for v = day^{-1}.

		Calcification	**Photosynthesis**	**Growth**
k_1 (pg C cell^{-1} day^{-1} or day^{-1})		-11.98	-17.68	-0.71
k_2 (μmol photons m^{-2}s^{-1})		-1.75E+06	-4.63E+06	-9.34E+05
k_3 (kg mol^{-1} μmol photons m^{-2}s^{-1})		6.43E+07	1.39E+09	3.10E+08
k_4 (mol kg^{-1} °C)		-0.22	-0.23	-7.28E-02
k_5 (°C)		28.14	26.72	-38.72
k_6 (kg mol^{-1} μmol photons^{-1} m^{2}s °C^{-1})		-3.09E+03	4.40E+03	-2.70E+03
R^2	(p-value)	0.7957 (<0.001)	0.7302 (<0.001)	0.8460 (<0.001)
F-value	(degrees of freedom)	389.51 (100)	273.52 (100)	552.74 (100)

Biogeosciences Discuss., https://doi.org/10.5194/bg-2018-88
Manuscript under review for journal Biogeosciences
Discussion started: 1 March 2018

Table 2. Optimum CO_2 concentrations, CO_2 $K\frac{1}{2}$ concentrations and maximum rates (V_{max}) at 10, 15 and 20°C from Eq. (2) fit to: CO_2-light data at 20°C in this paper and *E. huxleyi* CO_2 data from Sett et al. (2014) at 10°C, 15°C and 20°C and 150 μmol photons $m^{-2}s^{-1}$ light intensity. Note that the CO_2 working range for the equation for this species was 0-250 μmol kg^{-1}. Values exceeding this range were reported as >250 μmol kg^{-1}.

CO_2	**10°C**	**15°C**	**20°C**
CO_2 optima (μmol kg^{-1})			
Calcification	16.94	12.91	11.50
Photosynthesis	20.34	15.42	13.91
Growth rate	29.06	20.78	18.36
V_{max}			
Calcification (pg C cell^{-1} d^{-1})	6.37	8.94	9.69
Photosynthesis (pg C cell^{-1} d^{-1})	8.55	11.52	12.22
Growth rate (d^{-1})	0.59	1.08	1.38
$K\frac{1}{2}_{CO_2}$inhib μmol kg^{-1}			
Calcification	118.47	75.04	62.94
Photosynthesis	>250	119.54	100.51
Growth rate	>250	>250	192.74
$K\frac{1}{2}_{CO_2}$sat μmol kg^{-1}			
Calcification	1.66	1.56	1.48
Photosynthesis	1.65	1.50	1.42
Growth rate	0.85	1.19	1.40

Biogeosciences Discuss., https://doi.org/10.5194/bg-2018-88
Manuscript under review for journal Biogeosciences
Discussion started: 1 March 2018

Table 3. Optimum CO_2 concentrations, CO_2 $K\frac{1}{2}$ concentrations and maximum rates (V_{max}) at 50-1200 $\mu mol\,photons\,m^{-2}s^{-1}$ from Eq. (2) fit to: CO_2 data at 50, 400, 600 and 1200 $\mu mol\,photons\,m^{-2}s^{-1}$ and 20°C in this paper and *E. huxleyi* CO_2 data from Sett et al. (2014) at 150 $\mu mol\,photons\,m^{-2}s^{-1}$ light intensity and 10°C, 15°C and 20°C. Note that the CO_2 working range for the equation for this species was 0-250 $\mu mol\,kg^{-1}$. Values exceeding this range were reported as >250 $\mu mol\,kg^{-1}$.

CO_2	50 PAR	150 PAR	400 PAR	600 PAR	1200 PAR
CO_2 optima (μmol kg^{-1})					
Calcification	8.39	11.67	15.21	16.75	19.14
Photosynthesis	9.92	14.47	21.44	26.47	52.12
Growth rate	14.97	19.1	21.26	21.32	20.23
V_{max}					
Calcification (pg C cell^{-1} d^{-1})	7.64	10.05	12.47	13.48	15.04
Photosynthesis (pg C cell^{-1} d^{-1})	9.16	12.78	17.27	19.82	27.24
Growth rate (d^{-1})	1.19	1.43	1.58	1.61	1.62
$K\frac{1}{2}_{CO_2}$inhib μmol kg^{-1}					
Calcification	47.38	63.01	80.19	87.68	99.10
Photosynthesis	73.04	104.90	182.32	>250	>250
Growth rate	157.71	208.62	206.04	192.60	163.64
$K\frac{1}{2}_{CO_2}$sat μmol kg^{-1}					
Calcification	1.00	1.53	2.13	2.39	2.81
Photosynthesis	0.90	1.49	2.38	2.96	4.99
Growth rate	1.08	1.46	1.69	1.73	1.72

Biogeosciences Discuss., https://doi.org/10.5194/bg-2018-88
Manuscript under review for journal Biogeosciences
Discussion started: 1 March 2018

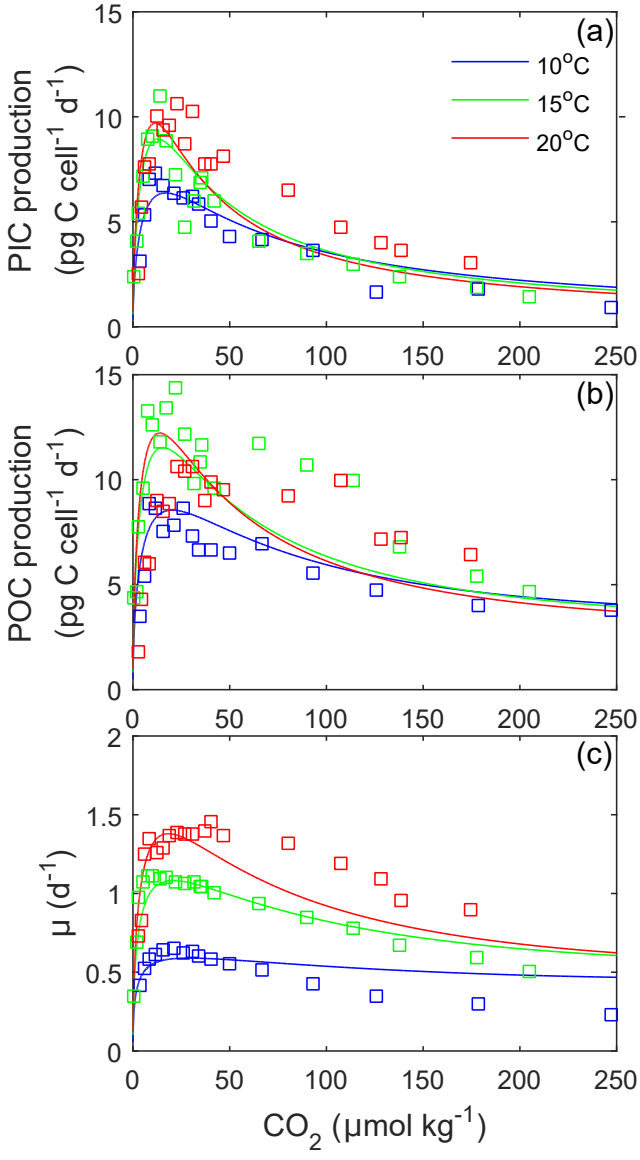

Figure 1. (**A**) Fitted particulate inorganic carbon (PIC), (**B**) particulate organic carbon (POC) production, and (**C**) growth rates (solid lines) in response to changes in carbonate chemistry at 10°C, 15°C and 20°C using Eq. (2) and fit coefficients from table 1. Symbols represent rate measurements from Sett et al. (2014) at 10°C, 15°C and 20°C and 150 μmol photons m^{-2}s^{-1}.

Biogeosciences Discuss., https://doi.org/10.5194/bg-2018-88
Manuscript under review for journal Biogeosciences
Discussion started: 1 March 2018

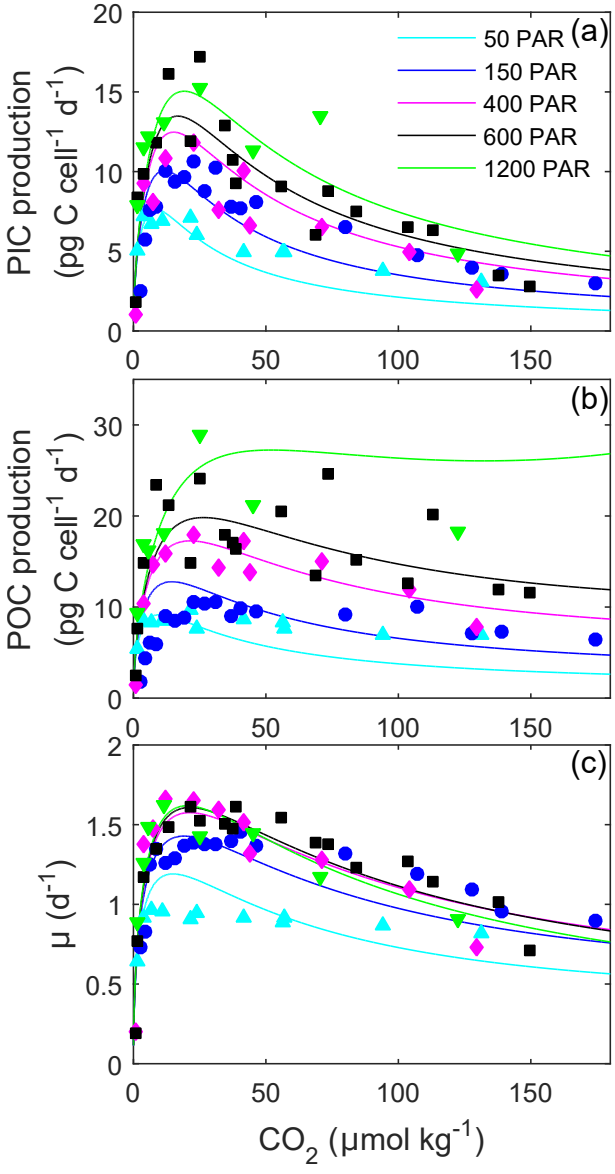

Figure 2. Fitted (solid lines) and measured (symbols) (**A**) particulate inorganic carbon (PIC) and (**B**) particulate organic carbon (POC) production, and (**C**) growth rates in response to changes in CO_2 concentration at six different light intensities using Eq. (2) and fit coefficients from table 1. Symbols represent rate measurements from this paper at a constant temperature (20°C) and 50, 150, 400, 600 and 1200 μmol photons m^{-2}s^{-1}.

Biogeosciences Discuss., https://doi.org/10.5194/bg-2018-88
Manuscript under review for journal Biogeosciences
Discussion started: 1 March 2018

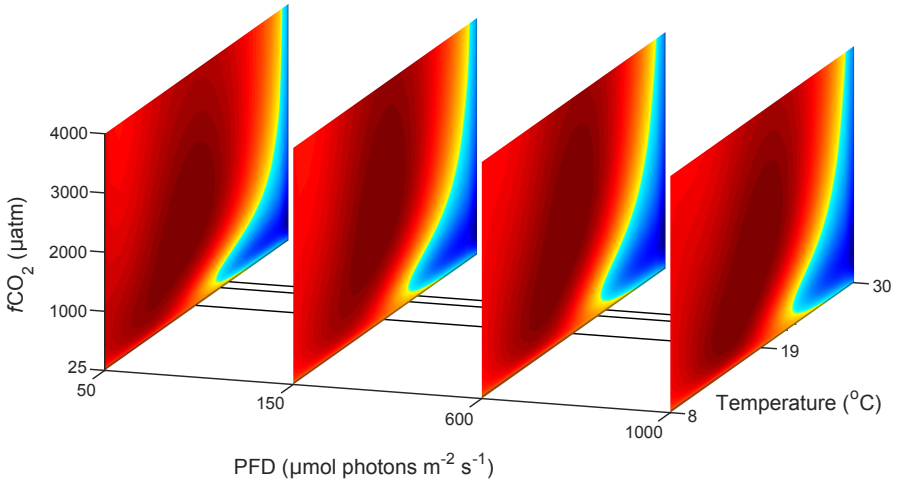

Figure 3. Predicted difference in growth rates between *Emiliania huxleyi* and *Gephyrocapsa oceanica* across a temperature range of 8-30°C and a fCO_2 range of 25-4000 μatm at 50, 150, 600 and 1000 μmol photons $m^{-2} s^{-1}$ of PAR based on Eq. (2). Note the response to varying CO_2 or temperature is not significantly influenced by light intensity.

Biogeosciences Discuss., https://doi.org/10.5194/bg-2018-88
Manuscript under review for journal Biogeosciences
Discussion started: 1 March 2018

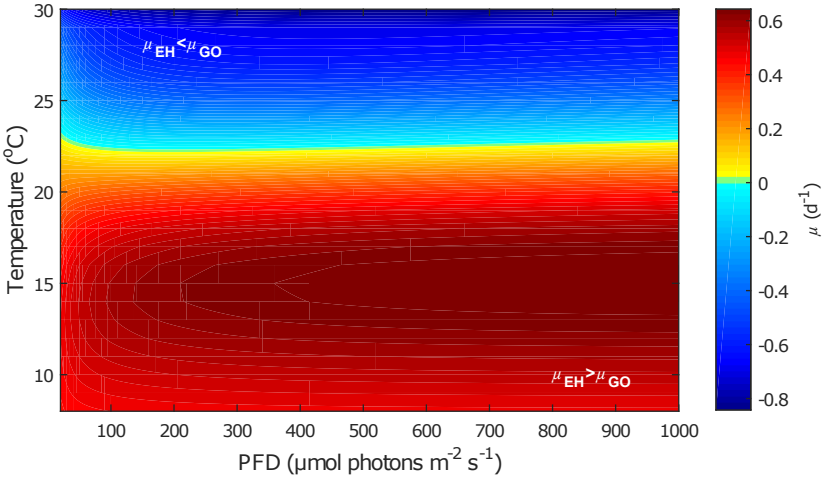

Figure 4. Predicted difference in growth rates between *Gephyrocapsa oceanica* and *Emiliania huxleyi* across a light range of 50-1000 $\mu\mathrm{mol\,photons\,m^{-2}s^{-1}}$ and a temperature range of 8-30°C at 400 $\mu\mathrm{atm}\,fCO_2$. based on Eq. (2).

Biogeosciences Discuss., https://doi.org/10.5194/bg-2018-88
Manuscript under review for journal Biogeosciences
Discussion started: 1 March 2018

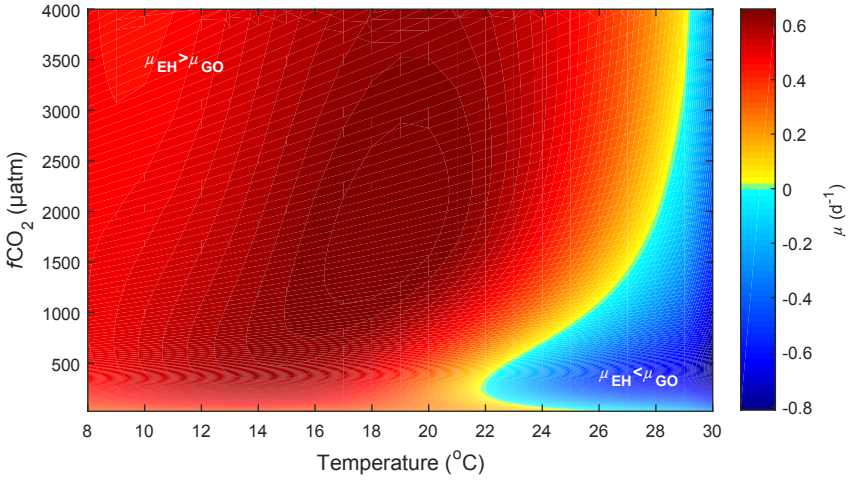

Figure 5. Predicted difference in growth rates between *Emiliania huxleyi* and *Gephyrocapsa oceanica* across a temperature range of 8-30°C and a fCO_2 range of 25-4000 μatm at 150 μmol photons $m^{-2}s^{-1}$ of light based on Eq. (2).

Biogeosciences Discuss., https://doi.org/10.5194/bg-2018-88
Manuscript under review for journal Biogeosciences
Discussion started: 1 March 2018

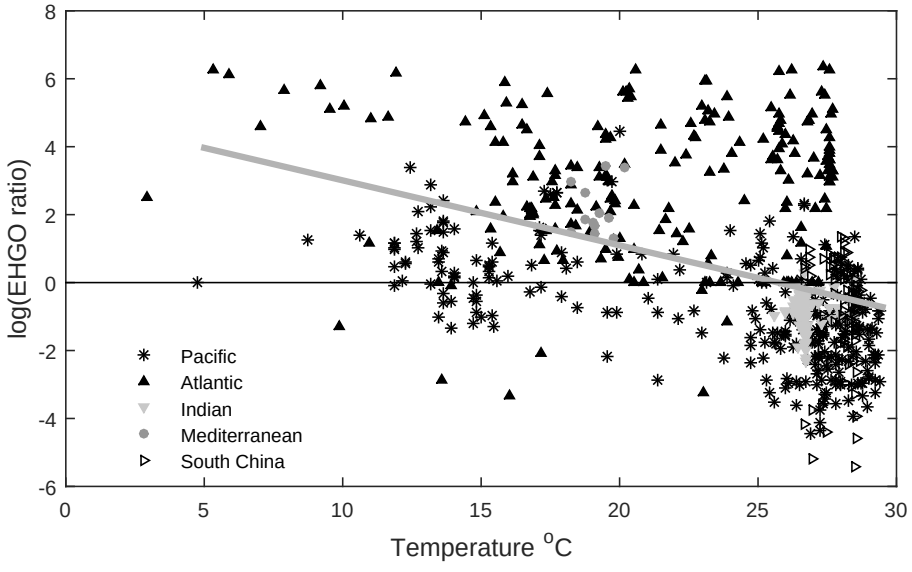

Figure 6. Log ratio of *E. huxleyi* to *G. oceanica* coccoliths versus temperature in the global oceans. Symbols and colours represent different ocean basins. The line at zero indicates a shift in dominance from *E. huxleyi* (>0) to *G. oceanica* (<0). The grey line represents a linear regression through the entire dataset with p<0.05 and F of 156.05. For details see Sect. 2.9.

Biogeosciences Discuss., https://doi.org/10.5194/bg-2018-88
Manuscript under review for journal Biogeosciences
Discussion started: 1 March 2018

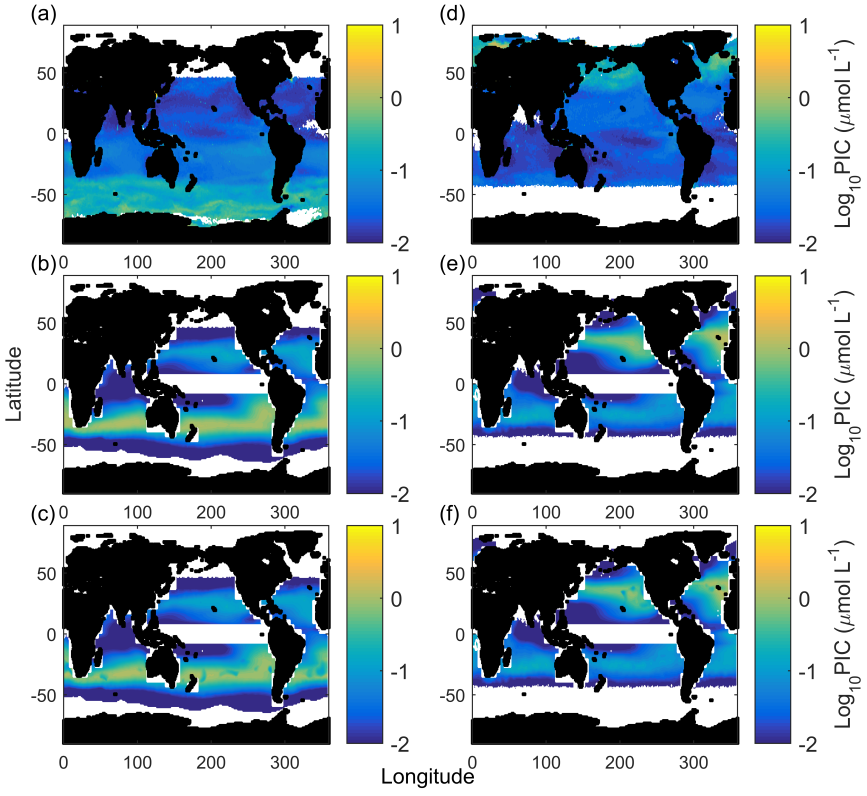

Figure 7. Austral summer/Boreal winter (**A**) and Austral winter/Boreal summer (**D**) satellite measured particulate inorganic carbon. Austral summer/Boreal winter (**B**) and Austral winter/Boreal summer (**E**) CCPP estimates accounting for carbonate chemistry (substrate and hydrogen ion concentrations), light intensity and temperature. Note the strong bands of CCPP at the mid-latitudes. Austral summer/Boreal winter (**C**) and Austral winter/Boreal summer (**F**) CCPP estimates accounting for carbonate chemistry (substrate and hydrogen ion concentrations), light intensity and temperature and nitrate concentrations (nutrient proxy).

Biogeosciences Discuss., https://doi.org/10.5194/bg-2018-88
Manuscript under review for journal Biogeosciences
Discussion started: 1 March 2018

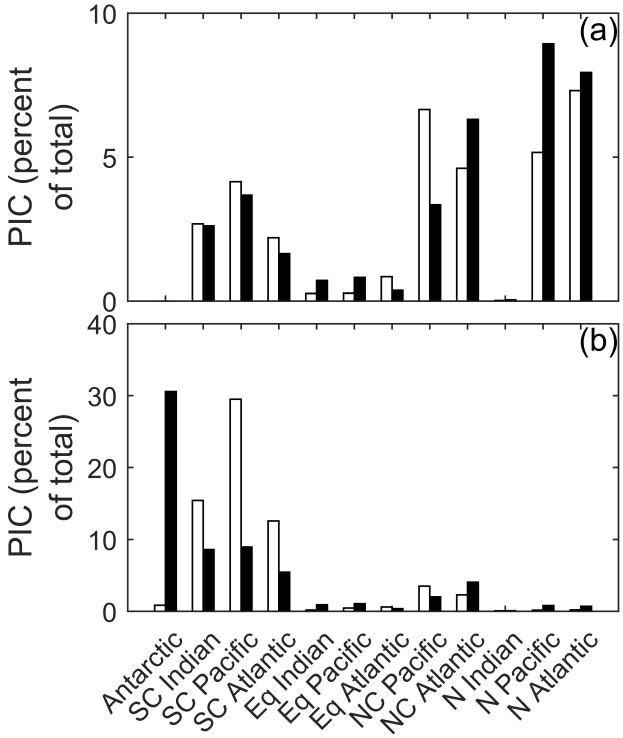

Figure 8. Satellite derived particulate inorganic carbon (black bars) and CCPP (white bars) estimates for major ocean biogeographical provinces (see figure S1 for details) as percentages of total production in (**A**) Austral winter/Boreal summer and (**B**) Austral summer/Boreal winter.